7-2008

Quantifying Antalgic Gait Knee Function Using Inertial Sensor Technology

William Mostertz
Clemson University, trippmostertz@gmail.com

QUANTIFYING ANTALGIC GAIT KNEE FUNCTION USING INERTIAL SENSOR TECHNOLOGY

A Thesis
Presented to
the Graduate School of
Clemson University

In Partial Fulfillment
of the Requirements for the Degree
Master of Science
Bioengineering

---

by
William Carl Mostertz, III
August 2008

Accepted by:
Dr. Lisa Benson, Committee Chair
Dr. Martine LaBerge
Dr. Steven Martin

ABSTRACT

The use of body-fixed inertial sensors to analyze human movement may prove useful in the medical field. Improving orthopaedic device design, diagnosing musculoskeletal disorders, and rehabilitation assessment could all benefit from a mobile gait analysis system based on inertial sensors. More specifically, patients recovering from lower limb corrective surgeries tend to adjust gait patterns to accommodate pain, a condition referred to as antalgic gait. Currently there is no quantitative method available to assess recovery for this patient population during post-operative management. A comparison of the inertial sensor system with the camera-based industry standard has confirmed it as a viable method for lower limb motion analysis during normal gait.

The inertial sensors consist of multiple accelerometers, gyroscopes and magnetometers used to obtain raw data, which is manipulated to calculate dynamic parameters. By comparing kinematic parameters between affected and unaffected limbs, it is possible to deduce a set of unique knee functionality ratios for recovering fracture patients. A control population was used to verify no significant difference ($p > 0.05$) of seven kinematic parameters between limbs during normal gait. Parameters included peak knee flexion-extension angles at $15 \pm 5\%$ and $75 \pm 5\%$ gait cycle. These parameters were then analyzed in a group of patients recovering from lower limb fractures, using the unaffected limb as a control/reference. The goal of this project is to use inertial sensor technology to pinpoint specific kinematic parameters of the lower limb that are clinically appropriate in assessing knee function of lower limb fracture patients during the post-operative time span critical in normal gait recovery.

DEDICATION

I would like to dedicate this manuscript to all of my friends and family that have supported and inspired me throughout my academic career. Thank you Amy, Barry, Ben, Brandon, Brian, Derek, Drew, Jeff, Joe, Kelly, Mickey, Nate, Nick, Sagar, Sara, and Sarah for all of the encouragement over the past several years. I would also like to thank Bryn Salter for always pushing me to be the best I can be, both intellectually and emotionally. I would especially like to thank my parents for their continuous support and love. Without you, I would have never become who I am today, thank you for always believing in me.

ACKNOWLEDGMENTS

I would like to acknowledge all those that have helped me along the way during my graduate career. I would like to acknowledge my committee members Dr. Martine LaBerge and Dr. Steve Martin. Thank you for your suggestions and guidance in completing my research. I would also like to acknowledge everyone at University Medical Group, Department of Orthopaedic Surgery, Greenville Hospital System, especially Stephanie Tanner and Dr. Kyle Jeray. Thank you for your patience and cooperation. A special acknowledgement is extended to everyone I have worked with in the Clemson University Biomechanics Lab: Josh Catanzarite, Aaron Koslin, Ryan Posey, Dr. John DesJardins, and Barry Hutto. Finally, I would like to give an enormous thank you to my advisor Dr. Lisa Benson. Thank you so much for giving me the opportunity to pursue my dreams.

TABLE OF CONTENTS

Page

Table of Contents (Continued)

Page

LIST OF TABLES

List of Tables (Continued)

LIST OF FIGURES

List of Figures (Continued)

Figure Page

CHAPTER ONE

INTRODUCTION

Background

Minimally invasive surgeries have become increasingly popular in the orthopaedic field. The desire to reduce surgical trauma, infection, and hospitalization length, yet still maintain a respectable post-operative aesthetic is conducted by minimizing the size and number of incisions during an operation. Arthroplasty is a common minimally invasive surgical procedure for orthopaedic surgeons to relieve pain and restore range of motion by realigning or reconstructing a defective joint. Joint replacement via arthroplasty has become the standard for most chronic knee problems, which can be attributed to the numerous advancements in artificial joint quality and type. Continuous developments of minimally invasive techniques and physical therapy regimens have significantly increased the quality of life in most patients. However, many individuals still experience an antalgic gait pattern, or adapted walking pattern to avoid pain, during the post-operative recovery period. This particular gait pattern is often non-ideal for fracture devices and can greatly reduce device lifespan and patient quality of life.

Post-operative evaluations of arthroplasty and other minimally invasive lower limb surgeries are recognized as an important means for judging patient recovery. Numerous scores and evaluations exist to assess the outcome of lower limb arthroplasties; however, due to clinician subjectivity and the lack of a universal standard, quantifying surgical results and subsequent recovery progress can be difficult. The most

common human physical activity is walking, which can be easily analyzed in a clinical setting. Quantitative gait analysis is generally accepted as an objective measurement of surgical success. The clinical use of gait analysis systems is effective in determining functional outcomes of lower limb corrective surgeries by their abilities to quantify the spatio-temporal parameters of walking and provide an overall assessment of physical capability in recovering patients [1-7]. However, typical clinical gait analysis systems are often expensive and require a dedicated staff and specialized facility to operate effectively. A solution should be capable of correlating objective gait data to the functional outcome of the patient, yet still operate conveniently and simply. A reliable post-surgical outcome assessment of patient activity and quality of life would be ideal.

Literature Review

The Gait Cycle – Normal vs. Abnormal

Normal gait is defined as an involuntarily coordinated musculoskeletal activity regulated by the nervous system that facilitates movement. Human ambulation is highly dependant on supraspinal systems. Biological areas responsible for proper gait have been identified in the brain stem, the basal ganglia, and thalamus. The cerebral cortex has also shown an important role in the initiation and correction of gait. Following initiation of motor activity, the central nervous system is responsible for the maintenance of balance and control via feedback through the cerebellum. Finally, vestibular and proprioceptive systems relay information for muscular adjustments of the lower limbs to occur [8, 9].

This complex reflexive system helps to maintain a dynamic equilibrium during normal gait.

A full gait cycle (Figure 1.1) describes the motions that occur between two heel strikes of the same limb. Once heel strike occurs, weight is gradually transferred across the sole from heel to toes. The contralateral foot is then simultaneously raised and accelerated. The upper body passes over the supporting leg causing the center of gravity to sway with each step. During ambulation, the upper body is held erect with the pelvis and shoulders at a level posture. Stance and swing phases divide the gait cycle and describe the basic actions of the involved limb. The stance phase begins with initial heel strike and ends with toe release (60% of cycle). The swing phase immediately follows stance and ends with next heel strike (40% of cycle) [10].

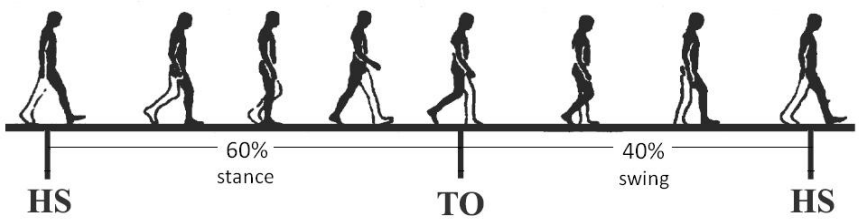

Figure 1.1: Illustration of a normal gait cycle. HS indicates heel strike and TO indicates toe-off events. Adapted from Herr and Wilkenfeld [11].

A variety of gait pathologies exist, all of which result from a multitude of conditions. Abnormal gaits are classified by their pathologic source. Neurologic gait pathologies include frontal gait, spastic hemiparetic gait, parkinsonian gait, cerebellar ataxic gait, and sensory ataxic gait. Abnormal gait patterns with combined neurologic

and musculoskeletal dysfunction include myelopathic gait, stooped gait of lumbar spinal stenosis, and steppage gait. Finally, gait patterns that result from only musculoskeletal abnormalities include coxalgic gait, Trendelenburg gait, knee hyperextension gait, and antalgic gait. Coxalgic and antalgic gait patterns typically result from osteoarthritis of the hip or knee respectively. However, antalgic gait can be seen in any individual with lower limb pain, including long-term degenerative joint diseases, ankle injuries, stress fractures, residual post-operative impairments, etc. [10].

Antalgic gait is defined as any gait pattern acquired as to reduce lower limb pain, typically the knee joint. This acquired gait pattern is characterized by a shortened time spent during the stance phase of the affected limb. During this reduced stance phase, the affected limb contacts the ground just long enough for the contralateral limb to initiate heel strike. This characteristic motion, or limp, minimizes the time of applied weight to the affected limb, thus reducing pain and discomfort [12]. Despite visual confirmation of a reduced stance phase on the affected limb, no quantitative data exists to define how the knee joint operates during antalgic gait. Moreover, antalgic gait can be further divided into chronic and acute gait patterns. Chronic antalgic gait is an adapted form that typically results from long-term degenerative joint diseases, such as knee osteoarthritis. Acute antalgic gait pertains to gait patterns acquired during the short post-operative time span of lower limb corrective surgeries critical for normal gait restoration. By evaluating knee function during this post-operative period, conclusions can be made about how to better manufacture fixation devices, or adjust physical therapy regimens, to stimulate a more effective gait recovery.

Knee Function Evaluations Following Arthroplasty and Other Lower Limb Reconstructive Surgeries

Various scoring systems and questionnaires have been used to evaluate lower limb functionality, specifically the knee joint, following surgery. The Hospital for Special Surgery Knee Score (HSS) is a knee functionality scoring system developed by Insall et al. [13]. This score incorporates several surgical procedural outcomes such as range of motion and alignment with subjective pain levels from the patient. A second score known as the Knee Society's Clinical and Functional Scoring System (KSS) was developed in 1989 [14]. This scoring system was similar to the HSS using many of the same surgical and subjective patient parameters. Both the HSS and KSS have been the basis for many studies involving the functional recovery of knee surgeries [15]. However, literature has indicated that these scores result in significant variability and present unreliable data for recovery assessment [16].

Despite the development of these scoring systems by surgeons and their extensive use in research, several disadvantages are present. Such disadvantages include patient subjectivity and low sensitivity to slight changes in functionality [16].

Instrumented Analyses of Knee Function – Gait Analysis

Gait analysis provides a non-invasive and convenient means for studying full body kinematics and kinetics over large data collection periods. Gait analysis has been used in several studies to assess functional outcome following surgical lower limb reconstruction [1-7]. It is also typical for gait analyses to be coupled with questionnaires when analyzing arthroplasty outcome [17, 18]. Three branches are associated in studying

gait: electromyography, kinetics, and kinematics. Revising conventional methods of measuring kinematics will be the focus of this study.

Gait Kinetics

Measurement of variant applied forces and moments during a gait cycle defines gait kinetics. These measurements are captured by a force plate embedded within a walkway. Past studies have shown that significant, negative changes occur to gait kinetics during the period immediately following knee arthroplasty [19]. Typically, kinetic gait parameters gradually improve; however, a greater rate of reduced walking pain is experienced prior to kinetic improvement. This may cause treatment regimens to become prolonged with undesirable outcomes due to subjectivity of patient pain tolerance with respect to proper kinetic gait recovery.

Gait Kinematics

Quantitative analysis of an ambulating body in space, without regard for the applied forces that produce motion, is referred to as gait kinematics. The most common form of kinematic gait data acquisition is by optical motion capture. Optical motion capture operates by using a set of infrared cameras that analyze the position of reflective markers attached to the study subject. This system has become a standard in human motion science and further providing beneficial assessment in orthopaedic-related disorders. Full systems are typically manufactured for medical specific applications that target areas of athletic performance, biomechanics, and gait analysis [20]. Such systems

include the VICON™ system, Elite™ system, Ariel™ system, and CODA™ system [21, 22]. All of these systems allow the collection and visualization of dynamic gait parameters during a variety of activities, including walking, running, and stair climbing.

Optical motion capture systems have limitations due to reflective marker attachment (i.e. markers are attached to skin surface rather than on physical bone). As a result, direct bone and joint kinematic parameters cannot be precisely measured. Therefore, accrued systemic errors can occur resulting in a significant lack in measurement confidence for knee orientation and rotations outside of sagittal measurements [23-26]. Moreover, optical motion capture systems are expensive and require committed laboratory space and staff. A stationary laboratory also results in non-ideal data capture scenarios. The subject must move in a restricted space, which limits motion capture to short distances and is furthermore assumed to be conducive to everyday patient activity.

Recent advances in micro-machined devices and sensor sensitivity have furthered the development of camera-free kinematic sensors and data capture methods [27-33]. Such kinematic sensors feed raw data into integrated algorithms and filters. These signals are then captured and delivered to an acquisition unit for processing. These sensors also have the advantage of being highly portable. They operate on battery power, measure parameters as body-fixed devices, and can transmit these parameters wirelessly to a host computer for analysis. These unique system characteristics allow for kinematic sensors to be a reliable substitute for optical motion capture. Body-fixed kinematic

sensors are less expensive, easier to use, and do not require committed laboratory space or trained staff.

Body-fixed sensors do, however, need to optimize the accuracy of three-dimensional kinematic readings by requiring an increased number of sensors. Increased sensor numbers hinders performance and creates an overall cumbersome system. An optimum number of kinematic sensors with reduced attachment sites, while maintaining the ability to sufficiently reproduce kinematic data representative of an ambulating body, would be ideal in gait analysis.

Inertial sensing is arguably the most extensive area of body-fixed kinematic sensing as it pertains to gait analysis. Inertial sensors are typically comprised of accelerometers and gyroscopes. These sensors can be designed to be sensitive up to all three axes of a Cartesian coordinate system that describes spatial movement. Recent developments in inertial sensor design have incorporated magnetometers to provide three-dimensional readings that indicate a magnetic north heading [31]. Using magnetometers in conjunction with accelerometers and gyroscopes, a local coordinate system can be effectively described within a global reference coordinate frame.

Conclusion

Many clinical scoring systems and questionnaires have been used to evaluate knee function following lower limb surgery. However, evaluation questionnaires present many limiting factors in their effectiveness. Main limitations include subjectivity, which is centered on the administrator's own bias and experience, and low sensitivity to minor

changes in pathological improvement. It is apparent that an objective instrument that utilizes keen detection devices to raise system sensitivity is a desirable tool for evaluation of lower limb function, specifically the knee joint, following surgery. Currently, optical motion capture is the most widely used and consistent technique in the quantization of surgical success of the knee. However, optical motion capture systems are complex and only accessible in select laboratories with expensive fixed cameras that require highly trained personnel. Furthermore, all of these drawbacks make recovery assessment very time-consuming and inconvenient for the patient.

This thesis proposes a novel method of ambulatory analysis to overcome these system limitations. The proposed system collects lower limb kinematic data from the patient by means of body-fixed inertial sensors. Specific system characteristics were repeatability, unobtrusiveness, portability, simplicity, and accuracy. All of these design features were modeled after the system's ability to continuously collect data during a full gait cycle. The end product is a sophisticated lower limb gait analysis system that produces individual spatio-temporal parameters, accelerations, angular velocities, and angles at the knee that define function. A hypothesis was developed that utilizes the previously described system and it states: kinematic similarities exist between normal left and right limb function, which would validate the use of the contralateral limb, within an acute antalgic gait population, as a reference to the affected limb. Furthermore, confirmed kinematic similarities can be used to develop functionality ratios that are clinically appropriate in assessing lower limb function during the post-operative time span critical in proper gait recovery.

CHAPTER TWO

INERTIAL SENSORS

Sensor Development and Refinement

Inertial sensor technology has undergone several advancements over the past decade [28, 34]. Sensors consisting of accelerometers and gyroscopes allow kinematic values such as thigh and shank orientations, and knee angles to be easily calculated [32, 33]. Angles and orientations are derived from the integration of translational accelerations, from accelerometers, and rotational velocities, from rate gyroscopes. However, many drawbacks have been associated with these calculations of kinematics. Integrated sensor signals are immediately distorted by drifts and offsets (attributed to soft tissue interference) and eventually become poor representations of true kinematic values [35]. Both electronic bias error and the deviation of sensor signals from their main sensing axis are main sources in drift associated with signal integration [36, 37]. Many attempts at correcting these errors have been made over the years. Initial efforts to capture gait kinematics made assumptions in ambulation, which resulted in equating sensor signals at the beginning and the end of a gait cycle [38]. More recent studies have applied heavy filtering techniques to the sensor signals at the expense of clipping kinematic data at lower frequencies [36].

Unique techniques have been developed to measure joint angles without the need to integrate sensor signals. However, these studies required multiple accelerometers and rate gyroscopes attached to external metal frames [39]. Using these devices was also found to be cumbersome for subjects.

State of the art advancements in inertial sensing have been accomplished by combining traditional accelerometer and gyroscope devices with a magnetic detection mechanism. Xsens Technologies B.V. (Enschede, The Netherlands) has developed a successful, drift free inertial sensor system by fusing triaxial accelerometers, gyroscopes, and magnetometers into a complex algorithm that calculates sensor position within a global reference frame [40]. The MTx™ inertial sensor (Xsens Technologies B.V., Enschede, The Netherlands) was selected to study the kinematics of the knee joint during normal and pathological gait. A brief overview of sensor mechanisms and design is described below.

Inertial Sensor Design

The MTx™ inertial sensor from Xsens Technologies B.V. is composed of three sensor modules that contribute to unrestrained orientation detection in a global coordinate system. The basic principle of how the MTx™ inertial sensor operates is as follows: A local vertical axis is determined by the accelerometer due to gravitational sensitivity. Vertical coordination is then horizontally stabilized by the detection of the global magnetic north via magnetometer. By continuous stabilization of the local coordinate frame, the gyroscopes are capable of obtaining drift-free orientation through a complimentary Kalman filter.

Accelerometers consist of a single mass suspended by a spring. These sensors operate on two physical principles: Hooke's law, $F = kx$, and Newton's second law of motion, $F = ma$. Equating these forces yields $F = kx = ma$, resulting in an acceleration

calculation of $a = \frac{kx}{m}$. A three-dimensional model can be developed by applying this system along three sensitive axes. Vibrating mass gyroscopes are used to measure angular motion within inertial sensor systems. When rotated, these continuously vibrating masses can detect a secondary vibration orthogonal to the sensitive direction. This phenomenon is known as the Coriolis Effect and allows for highly accurate rate of turn measurements [31].

Sensor Validation for Gait Analysis Applications

A previous study was conducted to confirm the kinematic comparability of inertial sensors to the gold standard, a camera-based motion analysis system. The inertial sensor system consisted of three uniaxial gyroscopes and a single, triaxial accelerometer. The entire inertial sensor system and the camera-based reflective markers were instrumented to right leg of seven subjects. Kinematic parameters of the lower limb were simultaneously collected for both systems. Parameters included knee flexion angle, angular velocities, and linear accelerations. Similarities were identified and found not statistically different, including an average maximum knee flexion angle difference of -2.5±7.7° during normal walking. The inertial sensor system was thus validated as a comparable alternative [41].

CHAPTER THREE

QUANTITATIVE LOWER LIMB KINEMATICS DURING ANTALGIC GAIT

Introduction

Gait Abnormalities – Antalgic Gait

Gait disorders typically stem from alterations of the nervous and musculoskeletal systems, and are primarily classified in three categories: neurologic, combined neurologic/musculoskeletal, and musculoskeletal. The majority of gait abnormalities exist in the elderly population with at least 20% of noninstitutionalized elderly individuals admitting to limited walking capabilities. One study indicates the prevalence of gait abnormalities in adults 85 and older to be over 54% [42].

A common musculoskeletal gait abnormality known as antalgic gait describes walking patterns that are acquired as to avoid or lessen pain [12]. Antalgic gait is defined by a characteristic shortened time span during stance phase of a single affected limb. This is due to the patient's attempt at quickly transferring body weight from the affected to the contralateral limb where a more bearable stance phase can be endured. Any condition that causes ambulatory pain of the lower limb, including degenerative joint diseases, stress fractures, ankle injuries, and post-operative lower limb trauma, may contribute to antalgic gait [43].

Antalgic gait patterns can be further divided into chronic and acute forms. Chronic antalgic gait patterns refer to those acquired as a result of a chronic condition, such as knee osteoarthritis. These adapted gait patterns tend to be more permanent and are difficult to fully restore. Acute antalgic gait describe gait patterns that are developed

following arthroscopy and many other lower limb corrective surgeries. In contrast to the chronic form, acute antalgic gait is typically short-lived and only exhibited during the post-operative time span critical for normal gait recovery.

Clinical Application

Physical therapy and surgical intervention are common treatments in reducing the severity of the antalgic gait disorder; however, residual impairment may remain long after fractures have healed. Nevertheless, determining treatments for antalgic gait is often a difficult task as there is currently no basis to quantify this particular pattern. Further complications arise in the ability to objectively distinguish between acute and chronic antalgic gait patterns. Despite visual confirmation of a reduced stance phase on the affected limb, no quantitative data exists to define how the knee joint operates during this acute form of antalgic gait. By evaluating knee function during this post-operative recovery period, conclusions can be made about how to better design fixation devices, or adjust physical therapy regimens, that would stimulate a more effective gait restoration. It is possible to study the kinematics of the knee joint, more specifically how the tibia rotates with respect to the femur, and develop functionality ratios using the contralateral limb as a control/reference. Previous studies have drawn comparisons between affected and unaffected limbs; however, ratios based on antalgic gait have not been developed [7]. Kinematic similarities exist between normal left and right limb function, which would validate the use of the contralateral limb, assuming it is unaffected functionally, as a reference to the affected limb within an acute antalgic gait population. Furthermore,

confirmed kinematic similarities can be used to develop functionality ratios that are clinically appropriate in assessing lower limb function during the post-operative time span critical in proper gait recovery.

This chapter describes the use of inertial sensor technology (MTx™ inertial sensors, Xsens Technologies B.V., Enschede, The Netherlands) to validate kinematic similarities between left and right limbs during normal gait. These similarities were then analyzed between affected and unaffected limbs of an acute antalgic gait population. Functional assessments and conclusions were developed based on the statistical findings.

Kinematic Data Collection

Figure 3.1 illustrates the MTx™ sensor coordinate system **S** within the global coordinate frame **G**. Rotations about x, y, and z axes are respectively defined as roll (angleϕ), pitch (angleθ), and yaw (angleψ)

.

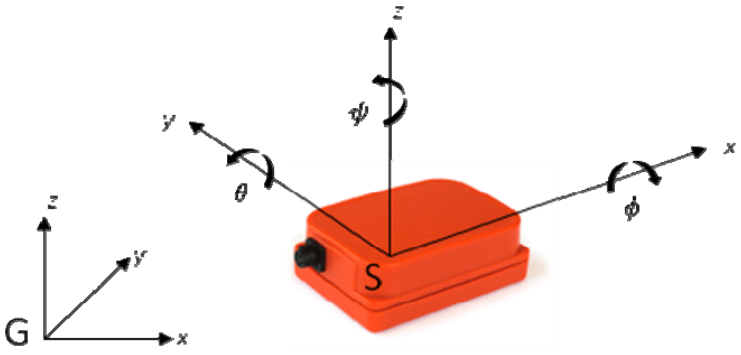

Figure 3.1: General representation of the MTx™ sensor coordinate system **S** with respect to a global coordinate system **G**.

The MTx™ inertial sensor uses rotation matrices to define orientation. Rotation matrices are commonly used to provide a complete representation of orientation within a global coordinate system. The rotation matrices are simply a collection of unit vector components from the sensor coordinate system **S** that are expressed in the global coordinate system **G**. When expressed in terms of Euler angles (ϕ,θ and ψ angles), the rotation matrix is thus:

$$ {}^{S}_{G}R = \begin{bmatrix} \cos\theta\cos\psi & \sin\phi\sin\theta\cos\psi - \cos\phi\sin\psi & \cos\phi\sin\theta\cos\psi + \sin\phi\sin\psi \\ \cos\theta\sin\psi & \sin\phi\sin\theta\sin\psi + \cos\phi\cos\psi & \cos\phi\sin\theta\sin\psi - \sin\phi\cos\psi \\ -\sin\theta & \sin\phi\cos\theta & \cos\phi\cos\theta \end{bmatrix} \quad (1) $$

$$ {}^{S}_{G}R = \begin{bmatrix} R_{11} & R_{12} & R_{13} \\ R_{21} & R_{22} & R_{23} \\ R_{31} & R_{32} & R_{33} \end{bmatrix} \quad (2) $$

Euler angles can then be calculated from the rotation matrices by the following calculations:

$$ \begin{aligned} {}^{S}_{G}\phi &= \tan^{-1}\left(\frac{R_{32}}{R_{33}}\right) \\ {}^{S}_{G}\theta &= -\sin^{-1}\left(R_{31}\right) \\ {}^{S}_{G}\psi &= \tan^{-1}\left(\frac{R_{21}}{R_{11}}\right) \end{aligned} \quad (3) $$

In order to obtain kinematic data that is representative of knee joint motion, a rotational relationship between the tibia and femur must be developed. Assuming that the thigh and shank operate as rigid bodies, the MTx™ inertial sensor can be securely attached and calculate real-time orientation of each segment. In order to determine relative rotation between the shank and thigh, the sensor coordinate frame of one segment must become the reference for the other segment coordinate frame. This is accomplished by developing an inverse rotation matrix. The inverse rotation matrix describes the rotations of the global coordinate frame within the sensor coordinate frame.

$$\left[{}^{S}_{G}R\right]^{-1} = {}^{G}_{S}R = \begin{bmatrix} R_{11} & R_{21} & R_{31} \\ R_{12} & R_{22} & R_{32} \\ R_{13} & R_{23} & R_{33} \end{bmatrix} \tag{4}$$

Rotation matrices of each segment are defined as thus:

$$\begin{aligned} R_{shank} &= {}^{shank}_{G}R \\ R_{thigh} &= {}^{thigh}_{G}R \end{aligned} \tag{5}$$

Relative rotation between the shank and thigh is calculated by developing a rotation matrix of how the shank rotates within the thigh coordinate frame. A unique rotation matrix describing this motion is calculated as follows:

$${}^{shank}_{thigh}R = {}^{G}_{shank}R\,{}^{thigh}_{G}R = \left[{}^{shank}_{G}R\right]^{-1}\,{}^{thigh}_{G}R \tag{6}$$

However, measuring rotation from the skin surface is not representative of how the femur and tibia rotate relative to each other at the knee joint. This limitation can be adjusted by translating the respective thigh/shank rotation coordinate frames to the center of knee rotation. Using anatomical references, a translational 4x1 matrix consisting of Cartesian displacements dx, dy, and dz is incorporated into each thigh/shank 3x3 rotation matrix. The result is a 4x4 transformation matrix that describes segment rotation at the knee joint center.

$$ {}^{S}_{G}T = \begin{bmatrix} & & & dx \\ & \left[{}^{S}_{G}R\right] & & dy \\ & & & dz \\ 0 & 0 & 0 & 1 \end{bmatrix} \tag{7} $$

Tibia and femur rotation matrices are now defined as:

$$ \begin{aligned} T_{tibia} &= {}^{tibia}_{G}T \\ T_{femur} &= {}^{femur}_{G}T \end{aligned} \tag{8} $$

Relative rotation between the tibia and femur is developed as previously described by calculating the rotation of the tibia within the femur coordinate frame.

$$ {}^{tibia}_{femur}T = {}^{G}_{tibia}T\,{}^{femur}_{G}T = \begin{bmatrix} & & & dx \\ & {}^{shank}_{G}R & & dy \\ & & & dz \\ 0 & 0 & 0 & 1 \end{bmatrix}^{-1} \begin{bmatrix} & & & dx \\ & {}^{thigh}_{G}R & & dy \\ & & & dz \\ 0 & 0 & 0 & 1 \end{bmatrix} = \begin{bmatrix} & & & dx \\ & {}^{thigh}_{shank}R & & dy \\ & & & dz \\ 0 & 0 & 0 & 1 \end{bmatrix} = T_{knee} \quad (9) $$

By extracting Euler angles from the resulting T_{knee} transformation matrix, three-dimensional knee function can be described (Figure 3.2). All calculations were adapted from previous studies using rotation matrices to estimate orientation [44, 45].

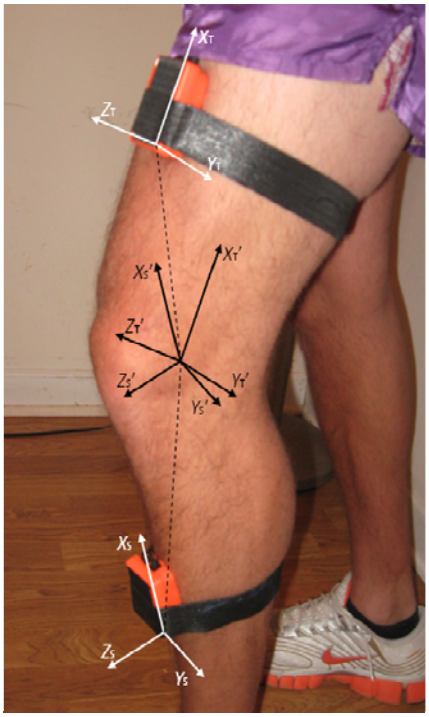

Figure 3.2: Basic principle of minimizing rotational error by translating coordinate systems to center of knee joint. X_T indicates x-axis of thigh and X_T' denotes x-axis of transformed coordinate frame.

In order to validate the capabilities of the MTx™ inertial sensor attachment scheme, a test rig was built to simulate the basic rotations of the knee joint (Figure 3.3). Sensors were attached to the rig and data was collected in a variety of positions. A goniometer fastened to the test rig was used to judge the accuracy of the sensor readings and software calculation adjustments were made accordingly.

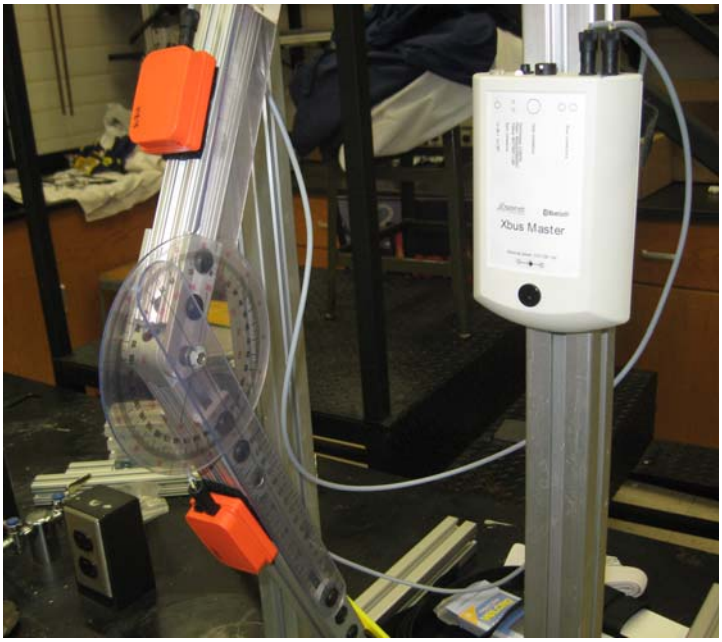

Figure 3.3: Simulated knee joint apparatus used in initial testing of sensor outputs and configuration.

Methods

Subject Selection

Control subjects (n=5) with no history of walking difficulty or impairment were selected to study the relationship between left and right unaffected limbs. Antalgic subjects (n=5) were selected based on the following criteria: recovering from an acute injury to the lower limb, visual confirmation of abnormal gait and reduced stance time on

the affected limb, and partial to full weight bearing during ambulation. The study protocol and subsequent amendments were all approved through Clemson University and the institutional review committee (IRC-A, Greenville Hospital System, Greenville, SC). All participants were asked to sign an approved informed consent form which outlined the purpose and methods of the study.

Instrumentation

Subjects were instrumented with two MTx™ inertial sensors. One was placed on the shank and the other on the thigh, both of which are fastened with Velcro® straps on the anterior aspect of the same limb. Sagittal and frontal plane pictures of the instrumented leg were taken (Figure 3.4).

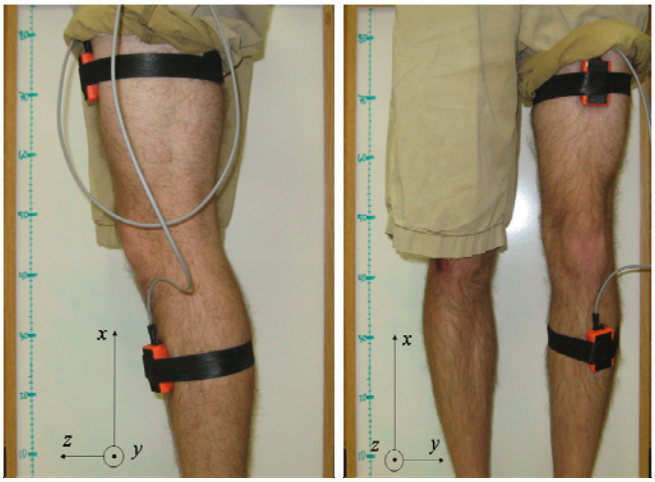

Figure 3.4: Sagittal and frontal views of instrumented control subject with length reference. Sensitive axes are indicated. x-axis, y-axis, and z-axis correspond to transverse, sagittal, and frontal plane rotations, respectively.

These were used to determine anthropometric distances between the sensors and the knee joint center of rotation, and were further implemented into transformation matrix calculations. Each sensor was then serially connected to the Xbus Master (Xsens Technologies B.V., Enschede, The Netherlands) wireless data acquisition unit, which was worn around the waist of the subject. The Xbus Master was then connected through a wireless Bluetooth™ network on a previously designated laptop COM port.

Data Collection

A laptop operated as the host system, which executed a master program developed using LabVIEW (National Instruments®, Austin, TX). The program collected live kinematic data from the attached inertial sensor devices. Once the master program was initiated the subject was asked to stand comfortably in front of an outlined walkway, ready to ambulate at a self-selected pace. A system wide calibration of the inertial sensor devices was performed while the subject retained a static, but comfortable stance. The subject was then asked to ambulate in a straight line while keeping a steady cadence. Data was collected at 120 Hz during the entire span of system calibration to the termination of the third gait cycle. This process was repeated to obtain a total of three trials on the affected limb. The sensors were then removed and placed in the same manner on the contralateral limb, and the same process was repeated as described previously. This includes shank and thigh sensor instrumentation and three trials of three gait cycles along a straight path.

Data Manipulation and Calculations

Photographs of both instrumented legs were analyzed in ImageJ, a publicly available image-processing program. Distances between sensor and knee joint center were estimated using an in-frame reference. These Cartesian-based distances were then applied to the 3x3 rotation matrices of each inertial sensor to form a 4x4 transformation matrix. The 4x4 transformation matrices indicate how each segment rotates in three-dimensional space at a new, translated origin. By translating the 3x3 rotation matrix of both the shank and thigh segments to the center of knee rotation, then relative rotation of the knee joint can be estimated. Equation 9 was used to develop a unique rotation matrix at the center of the knee joint that described relative rotation of the tibia within the femoral coordinate frame. Euler angles were calculated from this rotation matrix using the formulas from equation 3.

Internal-external rotation (ϕ rotation about the x-axis, transverse plane), flexion-extension (θ rotation about the y-axis, sagittal plane), and varus-valgus (ψ rotation about the z-axis, frontal plane) angles of the knee represented rotation about each axis. Angular velocities and linear accelerations of the thigh and shank were collected in triplicate for three gait cycles per limb as well. A full gait cycle was determined by observing a spike in acceleration along the vertical axis, which indicated a heel contact event. The second gait cycle for each trial was extracted by identifying these characteristic acceleration spikes and was further saved as a text file. Initiation and termination of gait were not considered due to inherent variability of gait balance and stability during these events [46]. Data sets (knee angles, angular velocities, and linear

accelerations) from each trial underwent spline interpolation in order to define values within a normalized percentage gait cycle parameter. Overall, twenty points were used, one reading per 5% gait cycle (GC). Figure 3.5 is a schematic that outlines each step of data manipulation clarifying how raw sensor data is interpreted as knee joint angles.

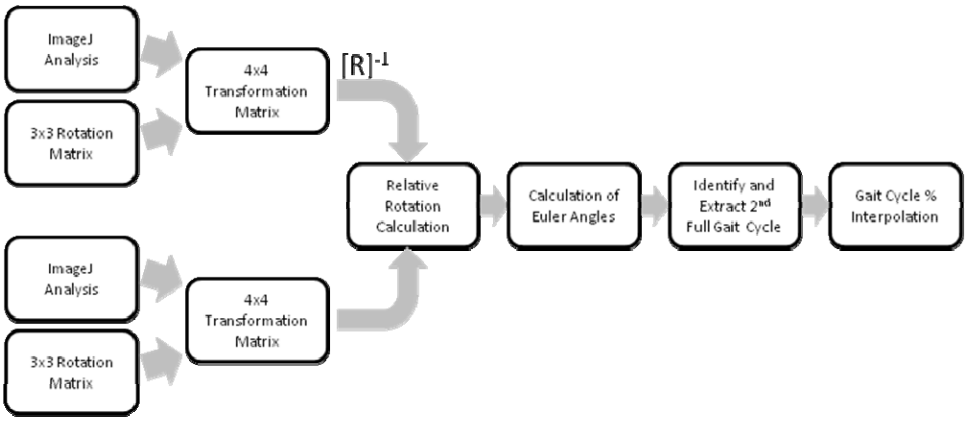

Figure 3.5: Work flow of data manipulation from 3x3 rotation matrices to percent gait cycle normalized kinematic parameters.

Comparing Data between Limbs

Each parameter was compared between left and right limbs on a comparison plot. Within the control population, comparable bilateral parameters were confirmed by plotting trendlines and identifying slopes near 1. Of these parameters, three were chosen based on more precise mean slope values between controls (knee flexion-extension angle, thigh sagittal rotation, and shank sagittal rotation). Next, kinematic points of interest were identified within chosen parameters by visual correlation at specific gait cycle percentages. A total of seven kinematic points of interest were chosen. Average maximum and minimum values for each kinematic point of interest were selected and

underwent a Student's t-test to validate no significant difference between parameters of both legs ($p > 0.05$). The seven validated control parameters were then applied to the acute antalgic gait population. A Student's t-test on average maximum and minimum peaks was used to compare parameters between affected and unaffected limbs. The parameters that indicated a significant difference were further used to develop functionality ratios (affected limb data divided by unaffected limb data) of the knee.

Results

Validating Method in a Control Population

Five control subjects completed three walking trials that consisted of three gait cycles on each limb. Knee angles and angular velocities of the left and right limbs were compared to each other (Figures 3.6 and 3.7). Slopes of each parameter for all control subjects are indicated in Table 3.1 with confirmed comparable parameters shaded yellow.

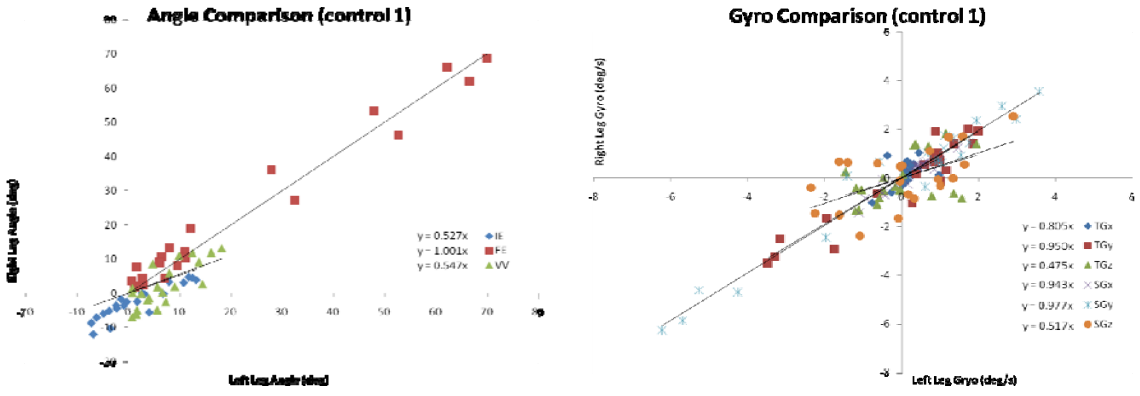

Figures 3.6 and 3.7: Comparison plots of knee joint angles and thigh/shank angular rotations for control subjects. Left (x -axis) and right (y -axis) kinematic parameters are plotted against each other. IE (internal-external rotation), FE (flexion-extension angle),

VV (varus-valgus angle), T (thigh), S (shank), Gx (transverse rotation), Gy (sagittal rotation), Gz (frontal rotation).

Table 3.1: Slopes from control subject comparison plots for each kinematic parameter. IE (internal-external rotation), FE (flexion-extension angle), VV (varus-valgus angle), T (thigh), S (shank), Gx (transverse rotation), Gy (sagittal rotation), Gz (frontal rotation). Comparable parameters are shaded yellow.

Subject	*Knee Angles*			*Thigh*			*Shank*		
	IE	FE	VV	TGx	TGy	TGz	SGx	SGy	SGz
Control 1	0.527	1.001	0.547	0.805	0.950	0.475	0.943	0.977	0.517
Control 2	0.456	1.008	1.058	0.688	0.876	0.868	0.167	1.083	0.535
Control 3	0.365	0.961	0.628	0.990	0.946	0.729	0.472	0.952	0.973
Control 4	0.854	0.977	0.534	0.887	0.823	0.685	0.540	0.889	0.903
Control 5	0.004	0.945	1.141	0.729	1.029	0.772	0.009	1.005	0.471
Mean	0.441	0.978	0.782	0.820	0.925	0.706	0.426	0.981	0.680
SD	0.306	0.026	0.294	0.122	0.079	0.146	0.362	0.071	0.238

Knee joint angles and thigh/shank angular velocities trials were graphed on a 100% gait cycle scale with data points per 5% gait cycle (Figures 3.8-3.10). Each plot contained three trials per sensitive axis (designated as IE, FE, VV or Gx, Gy, Gz).

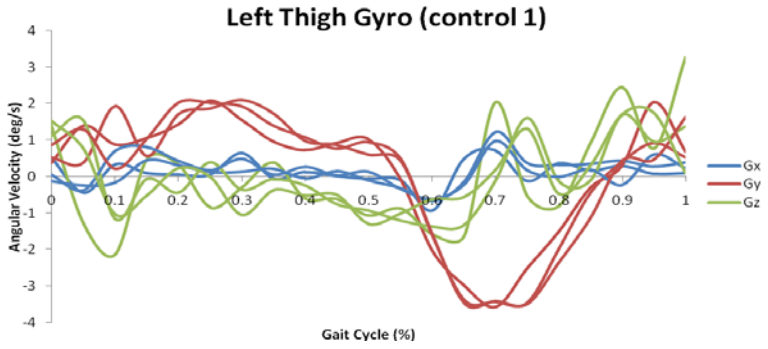

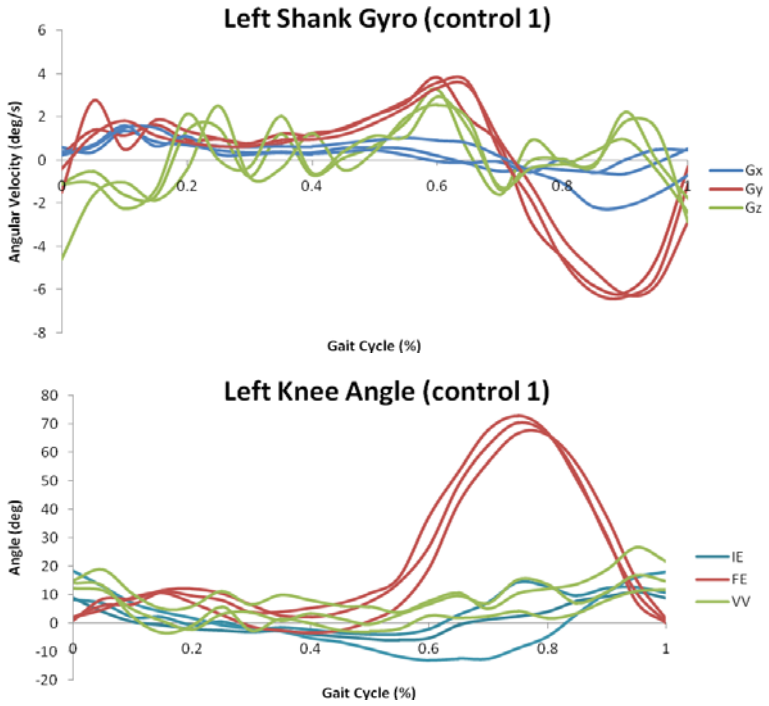

Figures 3.8-3.10: Left limb kinematic curves of a control subject for three trials. The data is normalized to 100% gait cycle. IE (internal-external rotation), FE (flexion-extension angle), VV (varus-valgus angle), Gx (transverse rotation), Gy (sagittal rotation), Gz (frontal rotation).

Mean curves of three trials per limb were developed for each kinematic parameter. Left and right mean curves were superimposed and similarities were observed in chosen parameters (Figures 3.11-3.13). Based on visual correlation, certain kinematic points were isolated from each curve. These kinematic points of interest were extracted at specific gait cycle percentages (±5%) and compared using an unpaired, 2-tailed Student's t-test to determine significant difference between limbs. A sample data analysis table for minimum knee flexion-extension angle is given below (Table 3.3).

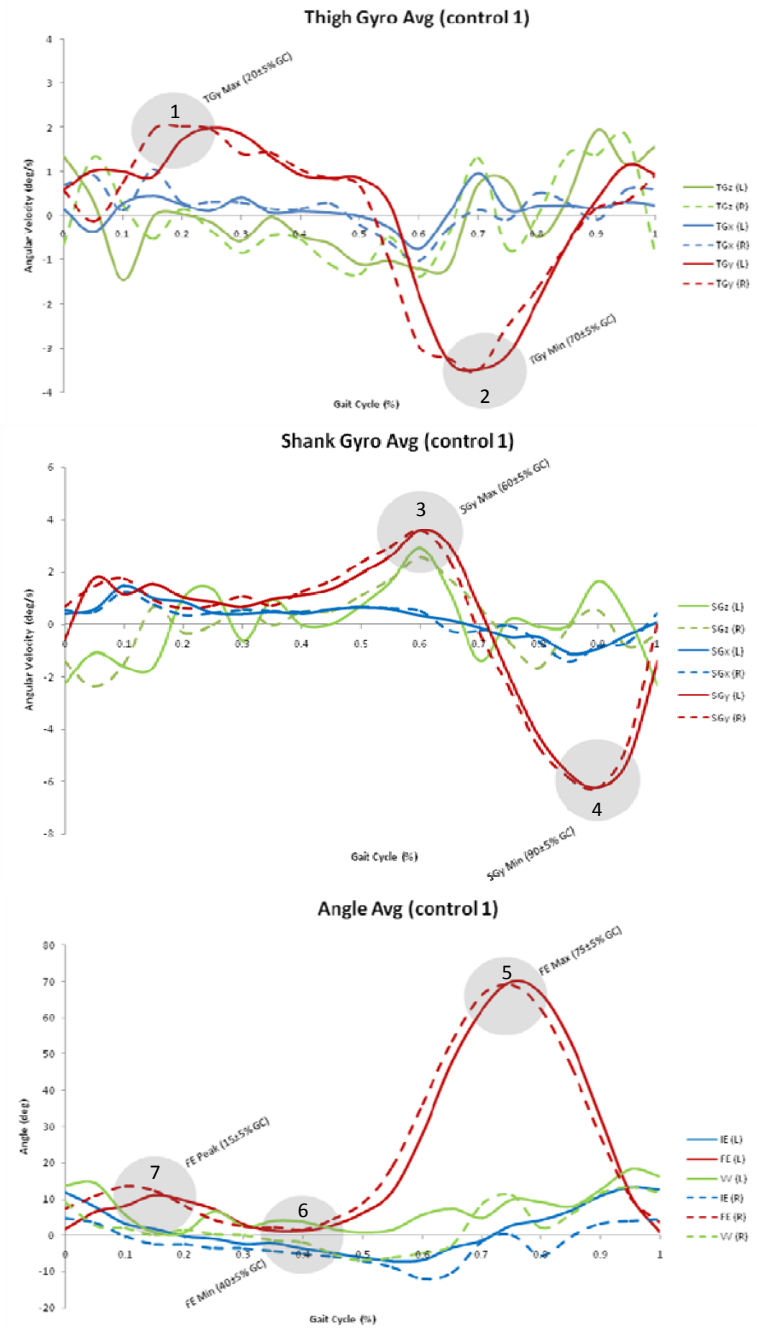

Figures 3.11-3.13: Superimposed left and right kinematic averages on a 100% gait cycle scale. Solid lines represent left limb data and dashed lines represent right limb data. IE (internal-external rotation), FE (flexion-extension angle), VV (varus-valgus angle), Gx (transverse rotation), Gy (sagittal rotation), Gz (frontal rotation). Shaded regions indicate the seven kinematic points of interest (Table 3.2).

Table 3.2: List of seven kinematic points of interest with numbered references to Figures 3.11-3.13 and Figures 3.21-3.23.

Kinematic Point of Interest	*Figure Reference*
TGy Max (20±5% GC)	1
TGy Min (70±5% GC)	2
SGy Max (60±5% GC)	3
SGy Min (90±5% GC)	4
FE Max (75±5% GC)	5
FE Min (40±5% GC)	6
FE Peak (15±5% GC)	7

Table 3.3: Student's t-test of minimum knee flexion-extension at 40±5% GC (gait cycle) for control 1. No significant difference ($p > 0.05$) was observed between parameter values of left and right limbs.

Control 1	***FE Min (40±5% GC)***	
	Left	Right
Trial 1	3.824	1.416
Trial 2	2.14	1.169
Trial 3	-3.409	1.742
Mean	0.852	1.442
SD	3.785	0.287
P Value	0.801	

A total of seven parameters were chosen at specific gait cycle (GC) percentages based on their statistical similarities between limbs (Table 3.2). Parameters included: Thigh Gy maximum at 20±5% GC, thigh Gy minimum at 70±5% GC, shank Gy maximum at 60±5% GC, shank Gy minimum at 90±5% GC, maximum knee flexion-extension angle at 75±5% GC, minimum knee flexion-extension angle at 40±5% GC, and peak knee flexion-extension angle at 15±5% GC. Table 3.4 outlines each parameter for all control subjects, including mean values for three trials of each limb, standard deviations, and p-values between averages.

Table 3.4: Seven kinematic points of interest used to confirm no significant difference between left and right limb motion in a control population.

Subject		*Left*	*Right*	*Left*	*Right*	*Left*	*Right*	*Left*	*Right*
		TGy Max (20±5% GC)		TGy Min (70±5% GC)		SGy Max (60±5% GC)		SGy Min (90±5% GC)	
Control 1	Mean	1.995	2.218	-3.504	-3.487	3.613	3.574	-6.225	-6.248
	SD	0.111	0.257	0.056	0.221	0.205	0.144	0.092	0.127
	P Value	0.239		0.904		0.804		0.810	
Control 2	Mean	1.590	1.592	-2.912	-2.642	2.508	2.511	-5.100	-5.411
	SD	0.042	0.081	0.072	0.164	0.236	0.084	0.253	0.106
	P Value	0.962		0.059		0.988		0.121	
Control 3	Mean	1.577	1.63	-2.862	-2.972	2.801	2.889	-6.241	-6.256
	SD	0.0924	0.173	0.127	0.205	0.058	0.060	0.367	0.280
	P Value	0.662		0.474		0.143		0.957	
Control 4	Mean	1.629	1.630	-3.035	-2.972	3.234	3.289	-6.707	-6.256
	SD	0.136	0.173	0.204	0.205	0.382	0.171	0.098	0.280
	P Value	0.996		0.727		0.831		0.058	
Control 5	Mean	2.198	1.867	-3.337	-3.718	3.215	3.069	-6.811	-6.711
	SD	0.071	0.257	0.392	0.096	0.062	0.112	0.284	0.189
	P Value	0.098		0.177		0.119		0.637	

Subject		*Left*	*Right*	*Left*	*Right*	*Left*	*Right*
		FE Max (75±5% GC)		FE Min (40±5% GC)		FE Peak (15±5% GC)	
Control 1	Mean	69.973	68.921	0.852	1.442	11.256	14.252
	SD	3.065	0.856	3.785	0.287	0.676	2.038
	P Value	0.598		0.801		0.073	
Control 2	Mean	51.837	52.737	3.668	4.305	17.937	20.221
	SD	0.884	1.967	0.398	0.740	2.090	1.063
	P Value	0.510		0.259		0.167	
Control 3	Mean	68.557	66.086	1.514	2.622	15.662	13.095
	SD	0.865	1.983	1.030	0.472	0.550	4.035
	P Value	0.119		0.166		0.336	
Control 4	Mean	67.204	66.086	2.574	2.622	16.211	13.095
	SD	0.669	1.983	0.350	0.472	2.349	4.035
	P Value	0.407		0.894		0.312	
Control 5	Mean	61.410	61.261	3.851	6.755	18.177	18.895
	SD	1.559	1.674	1.361	5.094	1.439	4.481
	P Value	0.916		0.394		0.805	

Bar graphs were developed for both knee joint angle parameters and thigh/shank angular rotation parameters which serve as another visual representation of parameter correlation (Figure 3.14 and 3.15).

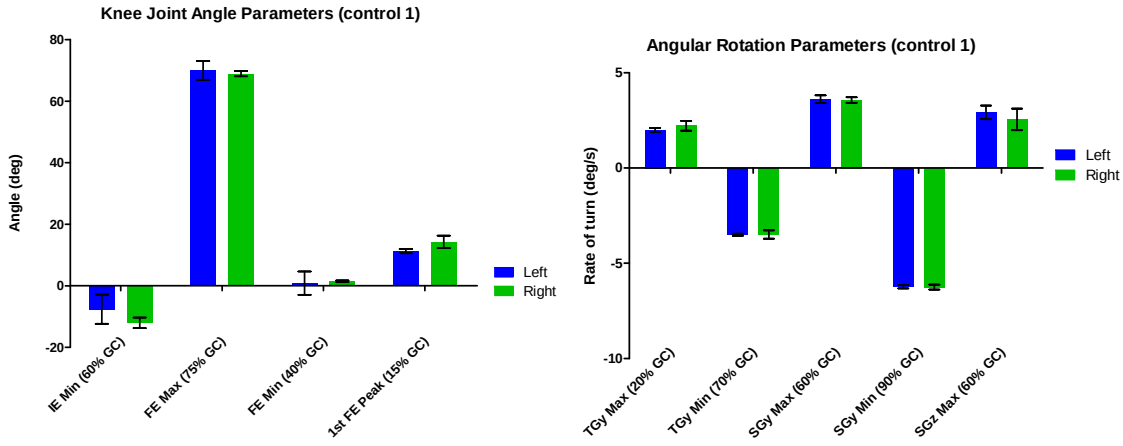

Figures 3.14 and 3.15: Bar graphs of knee joint angle and angular rotation parameters between left and right limbs in a control subject. Error bars indicate standard deviations.

Applying Method in an Acute Antalgic Gait Population

Five patients were selected based on acute antalgic gait criteria. Every patient had experienced a fracture below the knee on a single limb. All acute antalgic gait patients were in the full-weight bearing stage of gait recovery. Table 3.5 provides diagnostics for each acute antalgic gait patient including fracture site and type, fixative devices installed, post-operative time point, and symptoms during data collection.

Table 3.5: Patient descriptions in an acute antalgic gait population.

Subject	*Affected Limb*	*Fracture*	*Hardware*	*Post-op Time*	*Symptoms*
Patient 1	Right	Distal tibia	IM nail	2.5 months	Affected limb knee pain
Patient 2	Right	Crushed ankle	Plates and screws	2 months	Severe abnormal gait
Patient 3	Left	Midshaft tibia/fibula	IM nail	6 months	None
Patient 4	Right	Distal fibula	Plates and screws	6 months	None
Patient 5	Left	Midshaft tibia/fibula	IM nail	6 months	Contralateral knee pain

Acute antalgic gait subjects completed three walking trials that consisted of three gait cycles on each limb. Similarly to the control population, mean curves of three trials per limb were developed for each kinematic parameter: knee joint angles and segmental angular velocities (Figures 3.16-3.18).

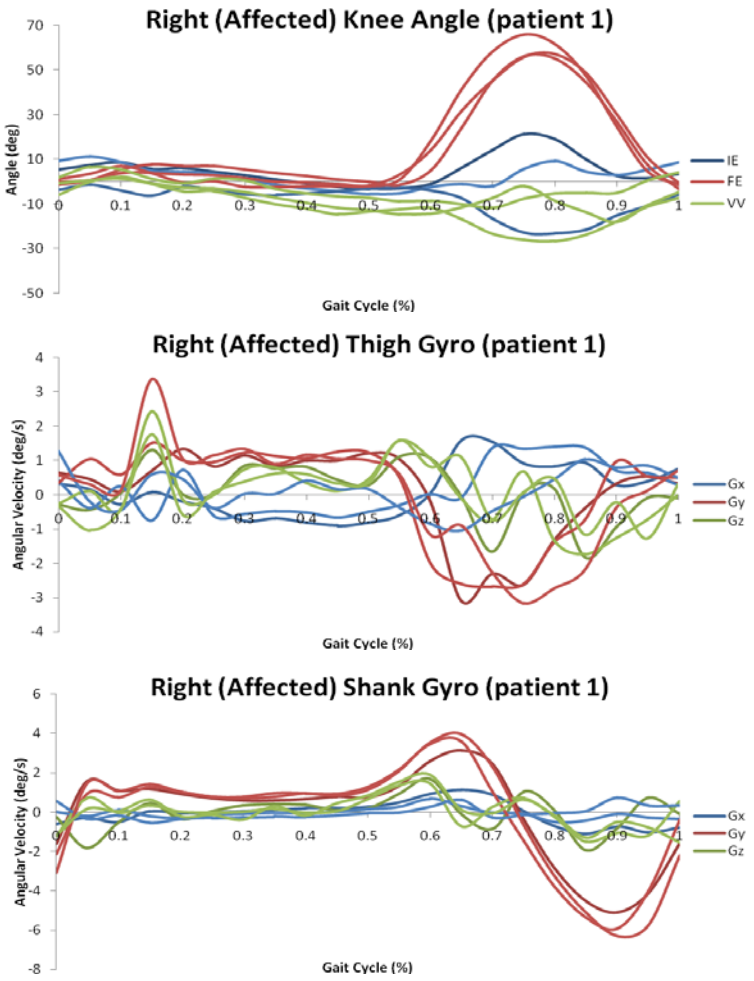

Figures 3.16-3.18: Affected limb kinematic curves of an acute antalgic patient for three trials. The data is normalized to 100% gait cycle. IE (internal-external rotation), FE (flexion-extension angle), VV (varus-valgus angle), Gx (transverse rotation), Gy (sagittal rotation), Gz (frontal rotation).

The seven previously validated kinematic points of interest, determined by the control population, were then extracted at the same percent gait cycle regions. Affected and unaffected limb parameters were then compared using an unpaired, 2-tailed Student's t-test. A sample parameter analysis is given in Table 3.6.

Table 3.6: Student's t-test of minimum knee flexion-extension at 40±5% GC (gait cycle) for patient 1. Significant difference ($p \leq 0.05$) was observed between parameter values of affected and unaffected limbs.

Patient 1	***FE Min (40±5% GC)***	
	Unaffected	Affected
Trial 1	4.884	1.089
Trial 2	8.665	-1.105
Trial 3	7.450	-2.212
Mean	6.999	-0.743
SD	1.930	1.680
P Value	0.006	

Table 3.7 outlines the seven validated kinematic points of interest for each acute antalgic gait patient, including mean values for three trials of each limb, standard deviations, and p-values between averages.

Table 3.7: Seven validated kinematic points of interest observed in an acute antalgic gait population. Red shading indicates a significant difference ($p \leq 0.05$) between parameter mean values of affected and unaffected limbs.

Subject		*Affected*	*Unaffected*	*Affected*	*Unaffected*	*Affected*	*Unaffected*	*Affected*	*Unaffected*
		TGy Max (20±5% GC)		TGy Min (70±5% GC)		SGy Max (60±5% GC)		SGy Min (90±5% GC)	
Patient 1	Mean	2.081	1.163	-2.980	-2.565	3.565	2.791	-5.777	-5.236
	SD	1.128	0.248	0.266	0.249	0.420	0.221	0.605	0.507
	P Value	0.240		0.120		0.048		0.301	
Patient 2	Mean	0.575	0.122	-1.814	0.607	1.960	0.069	-2.945	0.205
	SD	0.079	0.427	0.081	0.115	0.194	0.221	0.099	0.114
	P Value	0.145		7.581E-06		3.681E-04		3.490E-06	
Patient 3	Mean	2.600	2.188	-3.327	-3.540	2.824	3.267	-5.024	-6.153
	SD	0.266	0.376	0.173	0.666	0.202	0.608	0.556	1.579
	P Value	0.196		0.619		0.298		0.308	
Patient 4	Mean	1.714	1.831	-2.987	-3.030	2.759	2.393	-4.520	-5.201
	SD	0.097	0.227	0.047	0.164	0.142	0.283	0.348	0.740
	P Value	0.459		0.682		0.116		0.223	
Patient 5	Mean	1.422	1.404	-2.515	-2.986	2.540	0.758	-4.627	-1.529
	SD	0.393	0.382	0.128	0.203	0.296	0.097	0.452	0.149
	P Value	0.957		0.027		0.001		3.531E-04	

Subject		*Affected*	*Unaffected*	*Affected*	*Unaffected*	*Affected*	*Unaffected*
		FE Max (75±5% GC)		FE Min (40±5% GC)		FE Peak (15±5% GC)	
Patient 1	Mean	61.919	59.866	7.000	-0.743	14.706	6.337
	SD	4.597	5.418	1.930	1.680	3.199	2.090
	P Value	0.643		0.006		0.019	
Patient 2	Mean	11.215	35.262	14.043	4.466	25.528	10.285
	SD	2.292	2.627	1.32	2.756	3.22	2.134
	P Value	2.813E-04		0.006		0.002	
Patient 3	Mean	50.909	67.105	-5.824	2.504	14.526	15.635
	SD	3.257	12.419	0.835	2.097	1.857	3.082
	P Value	0.094		0.003		0.622	
Patient 4	Mean	50.452	51.219	1.698	-8.277	20.94	9.453
	SD	4.694	2.275	2.138	1.489	1.09	2.123
	P Value	0.811		0.003		0.001	
Patient 5	Mean	49.356	34.230	0.342	5.517	9.118	20.168
	SD	1.664	3.440	0.729	1.445	3.871	2.923
	P Value	0.002		0.005		0.017	

Finally, mean values from all seven kinematic points of interest were used to develop functionality ratios in a control population. Table 3.8 lists all seven functionality ratios for each control subject. Ratios were calculated by dividing left mean values by right mean values.

Table 3.8: Functionality ratios (left divided by right mean values) for all seven kinematic points of interest in a control population.

Subject		*Left*	*Right*	*Left*	*Right*	*Left*	*Right*	*Left*	*Right*
		TGy Max (20±5% GC)		TGy Min (70±5% GC)		SGy Max (60±5% GC)		SGy Min (90±5% GC)	
Control 1	Mean	1.995	2.218	-3.504	-3.487	3.613	3.574	-6.225	-6.248
	Ratio	0.899		1.005		1.011		0.996	
Control 2	Mean	1.590	1.592	-2.912	-2.642	2.508	2.511	-5.100	-5.411
	Ratio	0.998		1.102		0.999		0.942	
Control 3	Mean	1.577	1.630	-2.862	-2.972	2.801	2.889	-6.241	-6.256
	Ratio	0.967		0.963		0.970		0.998	
Control 4	Mean	1.629	1.630	-3.035	-2.972	3.234	3.289	-6.707	-6.256
	Ratio	1.000		1.021		0.983		1.072	
Control 5	Mean	2.198	1.867	-3.337	-3.718	3.215	3.069	-6.811	-6.711
	Ratio	1.177		0.897		1.048		1.015	

Subject		*Left*	*Right*	*Left*	*Right*	*Left*	*Right*
		FE Max (75±5% GC)		FE Min (40±5% GC)		FE Peak (15±5% GC)	
Control 1	Mean	69.973	68.921	0.852	1.442	11.256	14.252
	Ratio	1.015		0.590		0.790	
Control 2	Mean	51.837	52.737	3.668	4.305	17.937	20.221
	Ratio	0.983		0.852		0.887	
Control 3	Mean	68.557	66.086	1.514	2.622	15.662	13.095
	Ratio	1.037		0.577		1.196	
Control 4	Mean	67.204	66.086	2.574	2.622	16.211	13.095
	Ratio	1.017		0.982		1.238	
Control 5	Mean	61.410	61.261	3.851	6.755	18.177	18.895
	Ratio	1.002		0.570		0.962	

Bar graphs were developed for both knee joint angle parameters and thigh/shank angular rotation parameters which serve as a visual indication of significant difference between unaffected and affected limb parameters (Figure 3.19 and 3.20).

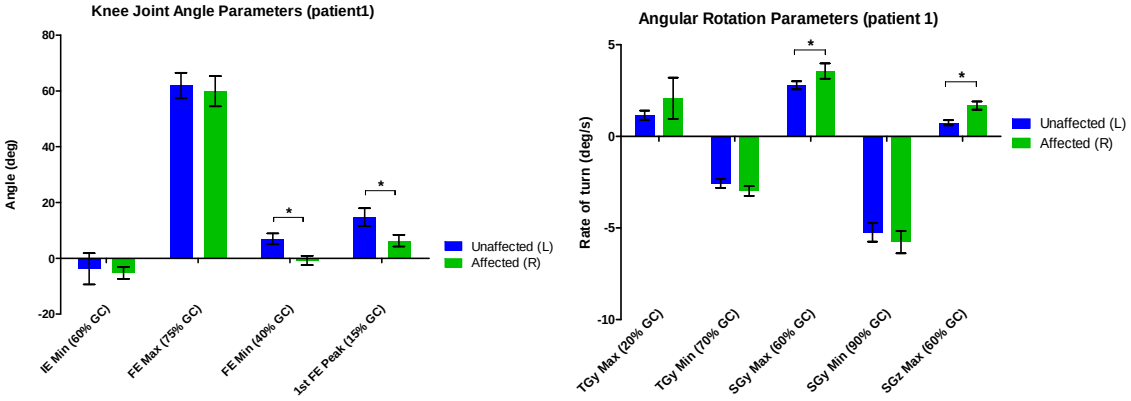

Figures 3.19 and 3.20: Bar graphs of knee joint angle and angular rotation parameters between unaffected and affected limbs in an acute antalgic gait patient. Error bars indicate standard deviations and * indicate a significant difference ($p \leq 0.05$).

Discussion

Control Population

Comparison plots are used to both validate correlation of data between limbs and identify potential functionality parameters for assessing kinematic knee function (Figures 3.6 and 3.7). Knee joint angles, shank/thigh angular rotations, and shank/thigh linear accelerations were compared between left and right limbs in subjects exhibiting normal gait. Comparing shank/thigh linear accelerations only confirms a steady-state progression through the gait cycle, and does not provide any information about how individual segments rotate. It should be noted that accelerations along the x-axis are strongly influenced by gravitational acceleration and are only used to identify a global coordinate system. For this reason, all linear accelerations were disregarded and only angular motions (shank/thigh angular rotations and knee joint angles) were considered in the study. A trendline was plotted across each data set and those with slopes close to 1

(FE, TGy, SGy) were considered when identifying candidate kinematic comparison parameters (Table 3.1).

In order to validate the use of the contralateral limb as a control/reference within an acute antalgic gait population, a statistical comparison needs to indicate no significant difference between left and right limb kinematic data of a normal, unaffected gait population. Superimposed left and right mean curves were used to visually extract seven 'kinematic points of interest' at specific gait cycle percentages (±5% GC) within comparable parameters that were previously confirmed with comparison plots. The shaded regions in Figures 3.11-3.13 indicate these seven kinematic points of interest. Each kinematic point of interest was compared between limbs using an unpaired, 2-tailed Student's t-test. All seven kinematic parameters were found to have no significant different ($p > 0.05$) between limbs. This comparison validated using a normal or unaffected limb as a control when studying gait patterns of unilaterally affected lower limb cases. Functionality ratios were then developed by divided left limb kinematic parameters with those of the right limb (Table 3.8). These functionality ratios ranged from 0.570 (control 5, FE Min (40±5% GC)) to 1.238 (control 4, FE Peak (15±5% GC)). Table 3.9 lists the range of appropriate functionality based on the findings in Table 3.8 and will be the basis of comparison in the acute antalgic gait population.

Table 3.9: Ranges for all seven functionality ratios developed from a control population.

Kinematic point of interest	*Functionality ratio range*
TGy Max (20±5% GC)	(0.899 – 1.177)
TGy Min (70±5% GC)	(0.897 – 1.102)
SGy Max (60±5% GC)	(0.970 – 1.048)
SGy Min (90±5% GC)	(0.942 – 1.072)
FE Max (75±5% GC)	(0.983 – 1.037)
FE Min (40±5% GC)	(0.570 – 0.982)
FE Peak (15±5% GC)	(0.790 – 1.238)

Acute Antalgic Gait Population

Superimposed graphs of kinematic data from unaffected and affected limbs indicate a great amount of variability between patients. However, all cases had at least one of the seven previously validated kinematic points of interest as significantly different ($p \leq 0.05$) between limbs (Table 3.7). Figures 3.21-3.23 are superimposed graphs of affected and unaffected kinematic data from patient 1 with kinematic points of interest indicated by shaded regions (references in Table 3.2). Visual differences in affected and unaffected kinematic parameters occur along the flexion-extension curve and at maximum and minimum values of angular shank rotation. In order to confirm reduced knee function, functionality ratios are developed. Table 3.10 is a functionality score card for patient 1 that compares individual functionality ratios (affected mean values divided by unaffected mean values) with those developed from the control population (Tables 3.8 and 3.9).

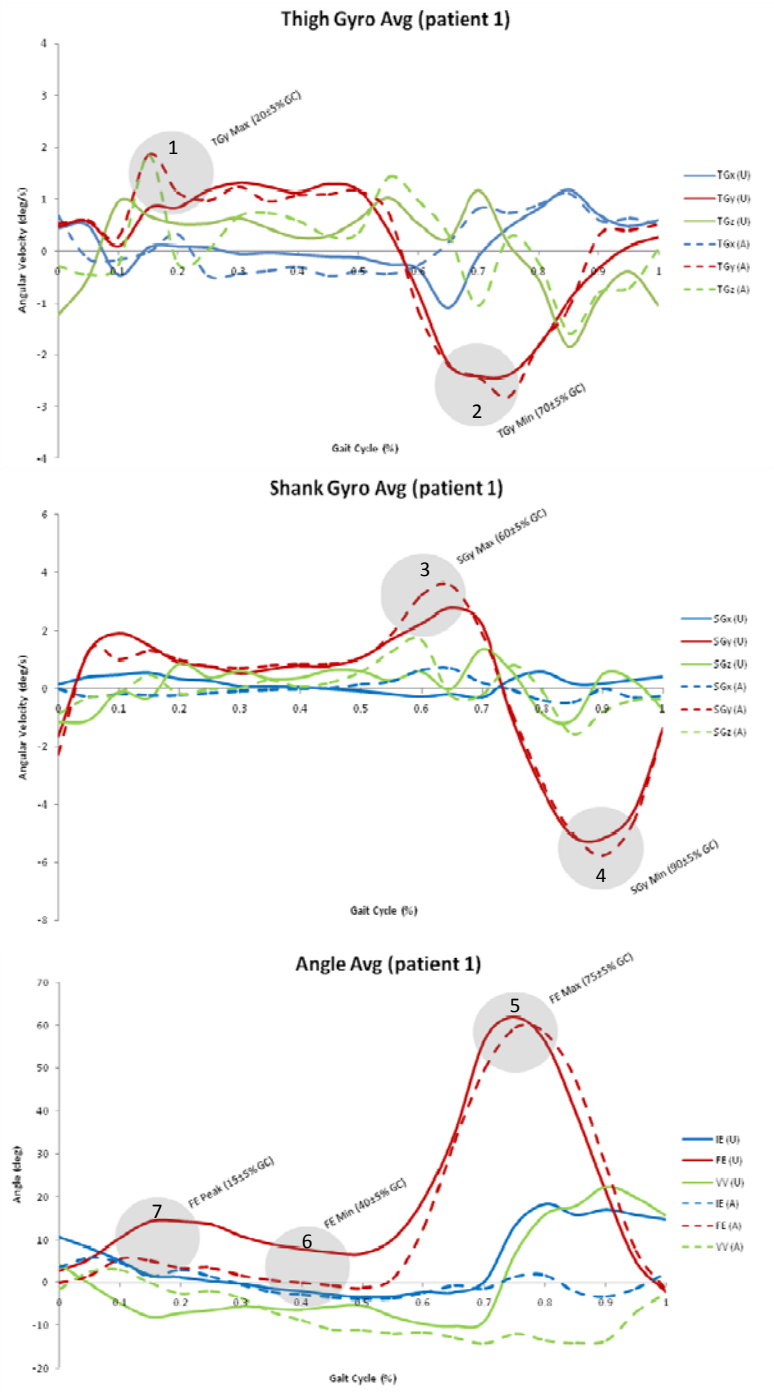

Figures 3.21-3.23: Superimposed unaffected and affected limb kinematic averages from patient 1. Solid lines represent unaffected limb data and dashed lines represent affected limb data. Shaded regions indicate kinematic points of interest (Table 3.2).

Table 3.10: Functionality ratio score card for patient 1. Red shading indicates parameters previously calculated as significantly different between limbs.

Patient 1		*Unaffected Limb (L)*	*Affected Limb (R)*	*Normal functional range*
TGy Max (20±5% GC)	Mean	1.163	2.081	
	Ratio	1.790		(0.899 – 1.177)
TGy Min (70±5% GC)	Mean	-2.565	-2.980	
	Ratio	1.162		(0.897 – 1.102)
SGy Max (60±5% GC)	Mean	2.791	3.565	
	Ratio	1.277		(0.970 – 1.048)
SGy Min (90±5% GC)	Mean	-5.236	-5.777	
	Ratio	1.103		(0.942 – 1.072)
FE Max (75±5% GC)	Mean	61.919	59.866	
	Ratio	0.967		(0.983 – 1.037)
FE Min (40±5% GC)	Mean	7.000	-0.743	
	Ratio	-0.106		(0.570 – 0.982)
FE Peak (15±5% GC)	Mean	14.706	6.337	
	Ratio	0.431		(0.790 – 1.238)

Patient 1 is an ideal case when trying to study knee function kinematics using the proposed contralateral limb comparison method. By sustaining an acute distal tibial shaft fracture, patient 1 demonstrated an antalgic gait pattern that inhibited knee motion without the influence of any other injured joint (i.e. ankle complex, hip). Theoretically, with no history of injury or pathology, the ability of patient 1's contralateral knee to function properly should be unaffected. A relatively short post-operative time span, 2.5 months, also indicates a critical point in normal gait recovery where adapted antalgic gait patterns may be permanent. It is during the 2-6 month post-operative range that affected knee function is the most prone to change. By relating mean values of the affected limb to the contralateral limb, functionality ratios of all previously validated kinematic points of interest are developed (Table 3.10). This functionality score card confirmed that all previously found, significantly different kinematic points of interest (red shading) were outside the normal range of proper knee function.

Regarding the entire acute antalgic gait study population, two parameters were of particular interest with at least four of the five patients exhibiting a significant difference between limbs. These included minimum flexion-extension angle at 40±5% GC and maximum flexion-extension angle at 15±5% GC. Minimum flexion-extension angle at 40% GC describes the highest angle of extension experienced between initial heel strike and toe-off events. Maximum flexion-extension angle at 15% GC represents the peak flexion angle immediately following initial heel strike. Table 3.11 lists functionality ratios for these selected kinematic points of interest.

Table 3.11: Knee functionality ratios calculated as affected mean value divided by contralateral mean value of kinematic points of interest.

Subject	*FE Min (40±5% GC)*	*FE Peak (15±5% GC)*
Patient 1	-0.106	0.431
Patient 2	0.318	0.403
Patient 3	-2.326	-
Patient 4	-4.875	0.451
Patient 5	0.062	0.452

The flexion-extension peak at 15% GC exhibited a high degree of repeatability, approximately 0.4 for four out of five patients. All four of these patients demonstrated a more conservative flexion-extension angle during stance phase when compared to that of the contralateral limb.

Another interesting finding is the consistent non-significant difference ($p > 0.05$) of maximum thigh angular velocity, about the y-axis, between the unaffected and affected thigh at 20% GC (Table 3.12).

Table 3.12: Comparison of maximum thigh angular rotation (*y* -axis) at 20% GC in an acute antalgic gait population.

Subject	TGy Max (20±5% GC)	
	P value	*Functionality ratio*
Patient 1	0.240	1.790
Patient 2	0.145	4.723
Patient 3	0.196	1.188
Patient 4	0.459	0.936
Patient 5	0.957	1.013

When considering a normal gait cycle, this particular parameter describes the rate at which the thigh rotates during stance phase. By not exhibiting a significant difference, it may be reasonable to disregard how the thigh independently rotates when analyzing lower limb kinematics of an acute antalgic gait population. However, non-significance may be attributed to the wide range of standard deviation and should be closely examined in future studies with larger populations.

Due to the high variability in knee functionality ratios it is obvious that studying knee kinematics with our methods of using the contralateral limb as a control is complex, and allows consideration of gait recovery on a case-by-case basis. For example, both patient 3 and patient 5 had sustained a midshaft tibia/fibula fracture and were 6 months post-operative. However, according to their score cards (Appendix B) patient 5 had considerably less knee functionality than patient 3. Despite both having the same fracture and post-operative recovery period, patient 5 had six significantly different kinematic parameters compared to the one exhibited by patient 3. This demonstrates the potential ability of this unique methodology to discriminate functionality between two seemingly identical acute antalgic gait cases.

CHAPTER FOUR

CONCLUSIONS AND FUTURE CONSIDERATIONS

The goal of this study was to examine the use of an inertial sensor system for assessing gait recovery in an acute antalgic gait population, and to identify specific kinematic parameters that can be used for this purpose. Also, the use of the contralateral limb as a control was studied, by comparing mean values between affected and unaffected limbs. Furthermore, in an attempt to quantify antalgic knee functionality, normal knee functionality ratios were developed from kinematic gait data observed in a control population.

Within an acute antalgic gait population, using the contralateral limb as a reference to the affected limb proved to be a beneficial method in studying the kinematic recovery of normal gait and knee function. This was validated by observing strong correlations between left and right kinematic parameters at certain points during a normal gait cycle, as well as identifying significant differences of these parameters in an acute antalgic gait population. It should be noted that all study methods and techniques were based on the assumption that the contralateral limb remains unaffected in functionality within an acute antalgic gait population.

Two kinematic parameters were of particular interest: maximum knee flexion at 15% GC and maximum thigh angular rotation about the sagittal plane (y -axis) at 20% GC. Maximum knee flexion at 15% GC of the affected limb was uniformly reduced when compared to contralateral knee flexion. Also, maximum thigh angular rotation in the sagittal plane was comparable between affected and unaffected limbs. Both findings

indicate an underlying kinematic knee function model that goes beyond the characteristic reduced stance phase of typical antalgic gait patterns.

Even though maximum knee flexion observed at 15% GC was consistently reduced in a general acute antalgic gait population, the majority of the seven kinematic points of interest were not reliable when developing knee functionality ratios. This is more than likely due to the many unique variables that characterize an individual gait cycle. After examining the results, some recommendations were developed to help refine this functionality ratio method and reduce variability. By increasing the number of attached sensors so that both legs were instrumented, an instantaneous relationship between affected and unaffected limbs of the same gait cycle can be developed rather than relating two separate cycles. A larger, more focused acute antalgic gait population may eliminate undesirable data readings when trying to develop a standard set of functionality ratios. For example, patient exclusion criteria may state that only 2-3 month post-operative proximal tibial fractures, that do not involve the tibial plateau, can participate in the study. Also, collecting data at a steady-state gait cycle, rather than the second gait cycle, may prove beneficial when determining key kinematic points of interest and refining normal functionality ratio ranges. Another study recommendation is to consider limb dominance when developing the normal functionality ratios (Table 3.8). Instead of arbitrarily dividing left and right mean values, determine limb dominance of the control subject and use mean values from the dominant leg as the normalizing factor. Regarding statistical analysis, a more rigorous comparison needs to be conducted between unaffected and affected limbs. Rather than comparing mean values at specific

gait cycle percentages, statistical analysis should consider the entire 100% gait cycle range between unaffected and affected kinematic parameters. Such analyses include the bootstrap method and the Gaussian point-by-point method [47]. Finally, future studies should incorporate kinetic measurements (forces and moments) of the knee into the overall kinematic assessment of normal gait recovery. Observing simultaneous kinematic and kinetic parameters at the knee allows for a complete lower limb profile to be developed and analyzed.

APPENDICES

Appendix A

Control Data

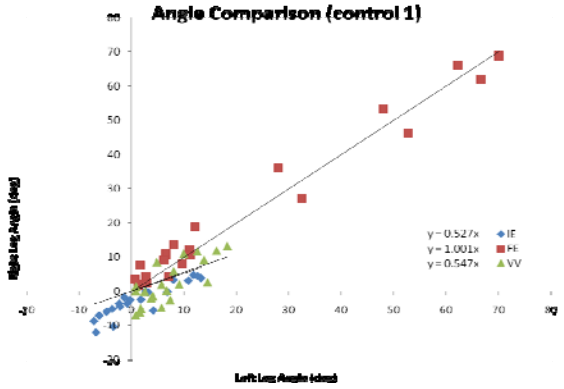

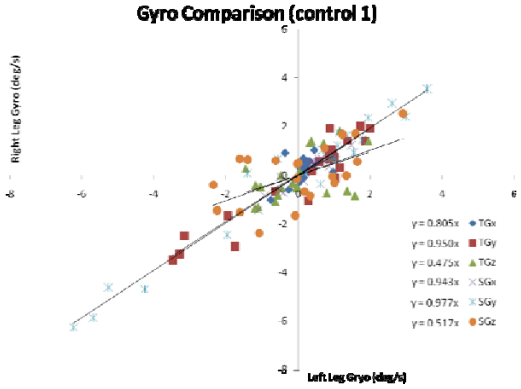

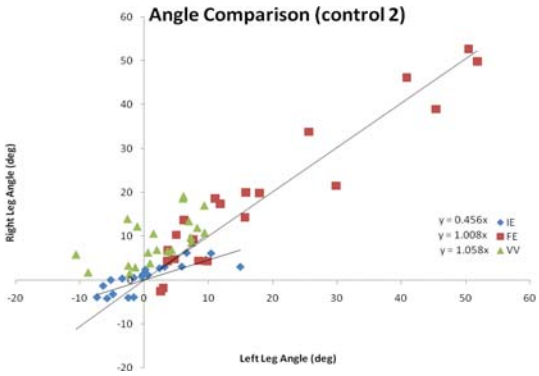

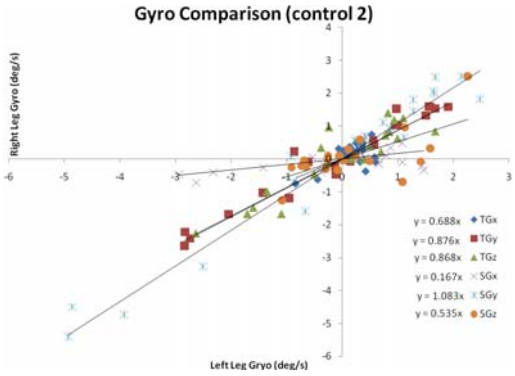

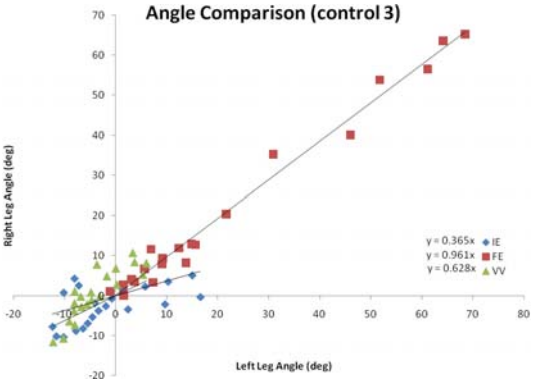

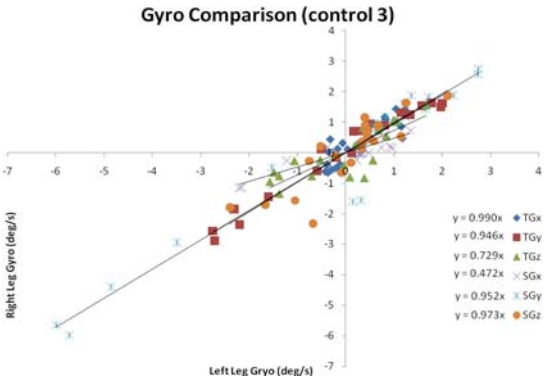

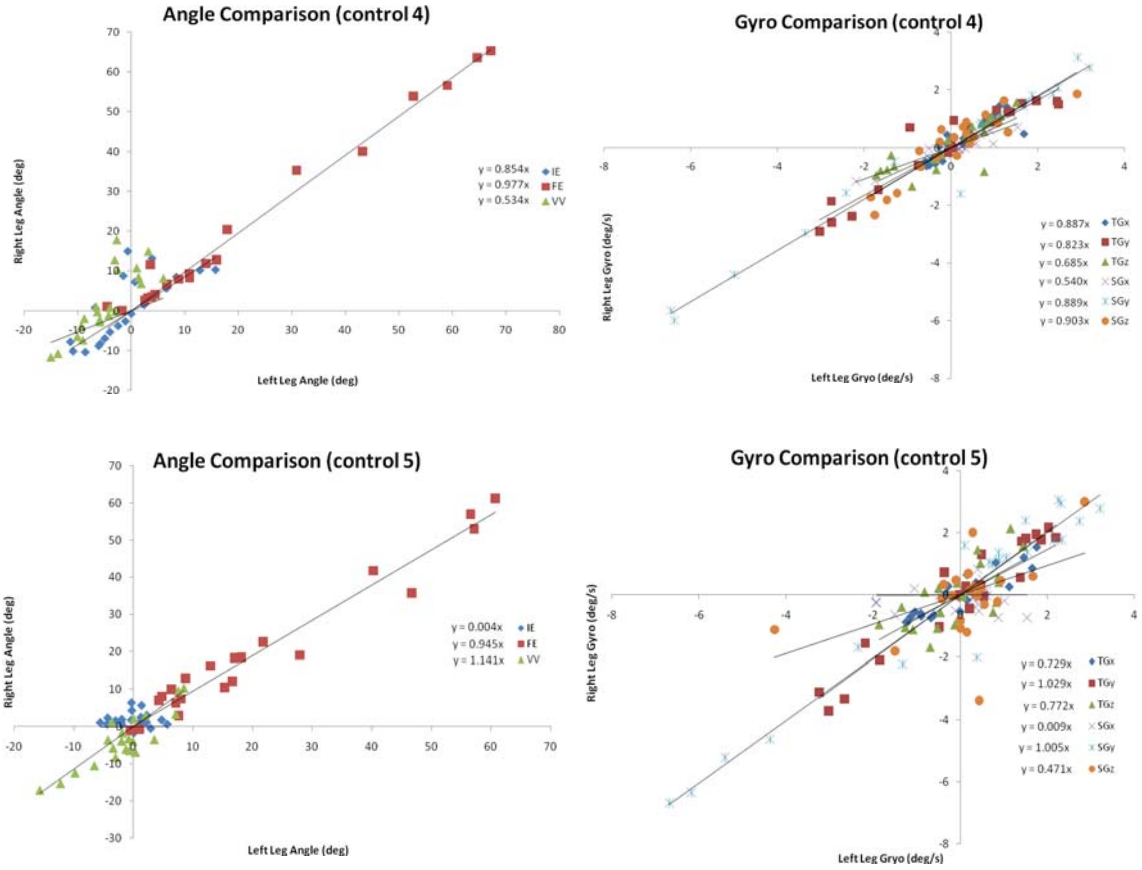

Figures A1-A10: Comparison plots of knee joint angles and thigh/shank angular motions. IE (internal-external rotation), FE (flexion-extension angle), VV (varus-valgus angle), T (thigh), S (shank), Gx (transverse rotation), Gy (sagittal rotation), Gz (frontal rotation).

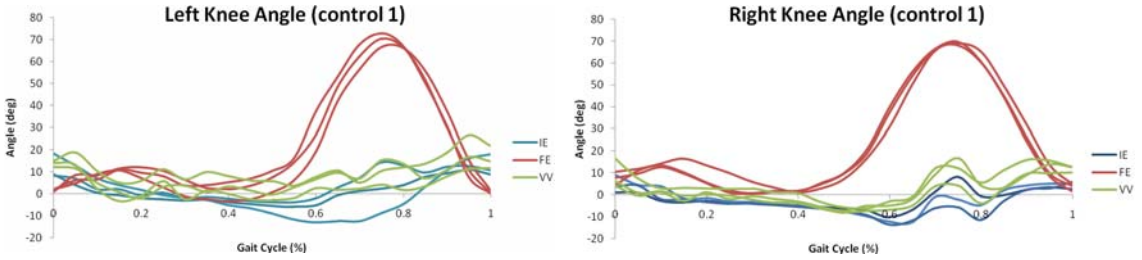

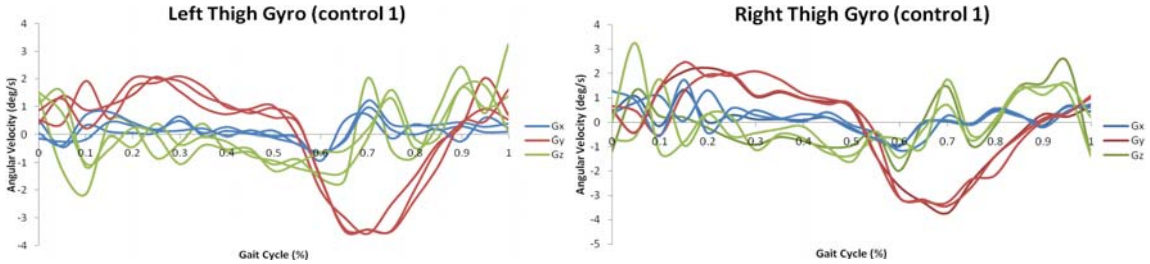
Left Thigh Gyro (control 1)
Angular Velocity (deg/s)
Gait Cycle (%)
Gx
Gy
Gz

Right Thigh Gyro (control 1)
Angular Velocity (deg/s)
Gait Cycle (%)
Gx
Gy
Gz

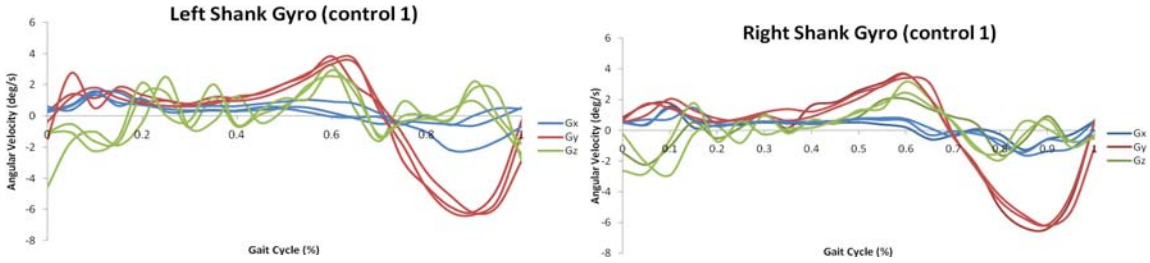
Left Shank Gyro (control 1)
Angular Velocity (deg/s)
Gait Cycle (%)
Gx
Gy
Gz

Right Shank Gyro (control 1)
Angular Velocity (deg/s)
Gait Cycle (%)
Gx
Gy
Gz

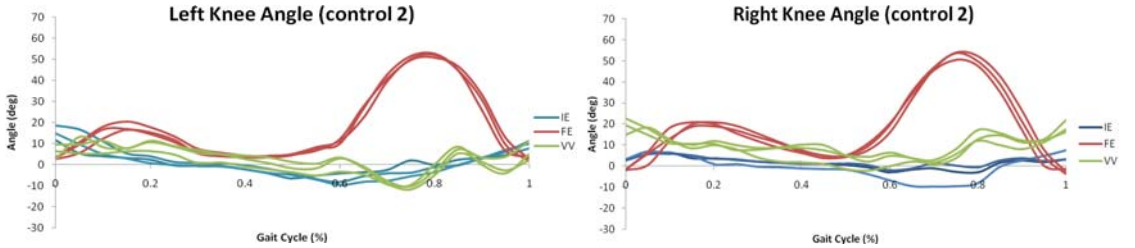
Left Knee Angle (control 2)
Angle (deg)
Gait Cycle (%)
IE
FE
VV

Right Knee Angle (control 2)
Angle (deg)
Gait Cycle (%)
IE
FE
VV

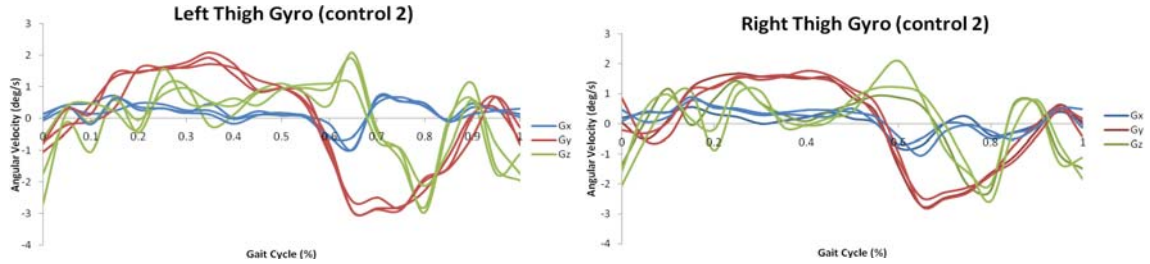
Left Thigh Gyro (control 2)
Angular Velocity (deg/s)
Gait Cycle (%)
Gx
Gy
Gz

Right Thigh Gyro (control 2)
Angular Velocity (deg/s)
Gait Cycle (%)
Gx
Gy
Gz

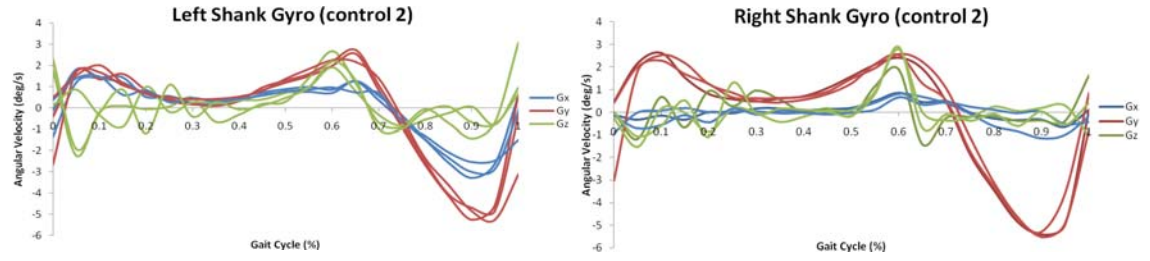
Left Shank Gyro (control 2)
Angular Velocity (deg/s)
Gait Cycle (%)
Gx
Gy
Gz

Right Shank Gyro (control 2)
Angular Velocity (deg/s)
Gait Cycle (%)
Gx
Gy
Gz

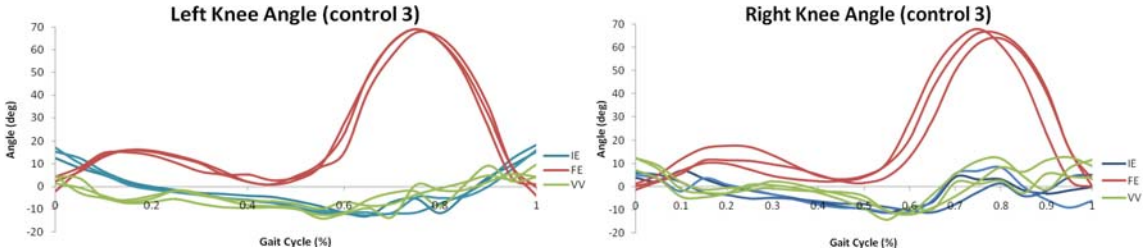
Left Knee Angle (control 3)
Angle (deg)
Gait Cycle (%)
IE
FE
VV

Right Knee Angle (control 3)
Angle (deg)
Gait Cycle (%)
IE
FE
VV

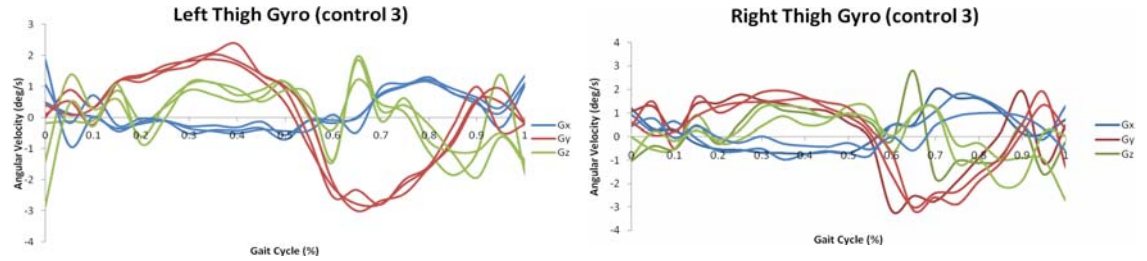
Left Thigh Gyro (control 3)
Angular Velocity (deg/s)
Gait Cycle (%)
Gx
Gy
Gz

Right Thigh Gyro (control 3)
Angular Velocity (deg/s)
Gait Cycle (%)
Gx
Gy
Gz

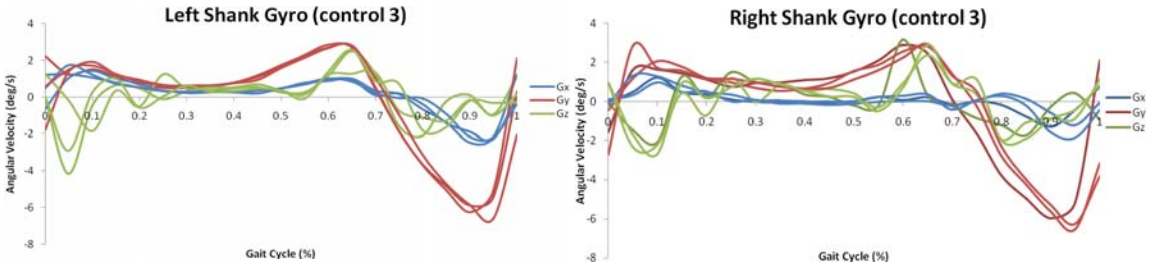
Left Shank Gyro (control 3)
Angular Velocity (deg/s)
Gait Cycle (%)
Gx
Gy
Gz

Right Shank Gyro (control 3)
Angular Velocity (deg/s)
Gait Cycle (%)
Gx
Gy
Gz

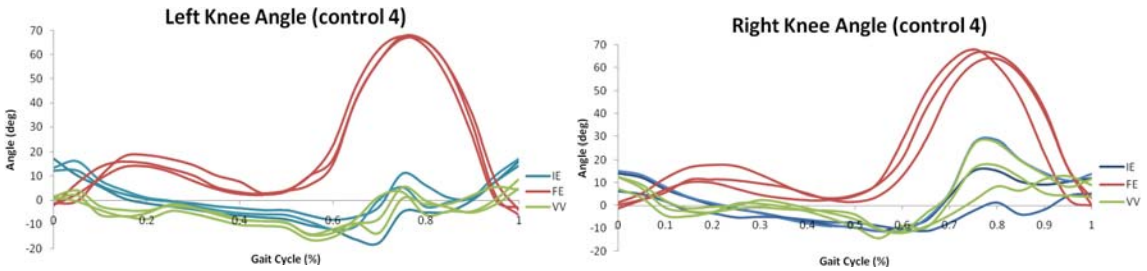
Left Knee Angle (control 4)
Angle (deg)
Gait Cycle (%)
IE
FE
VV

Right Knee Angle (control 4)
Angle (deg)
Gait Cycle (%)
IE
FE
VV

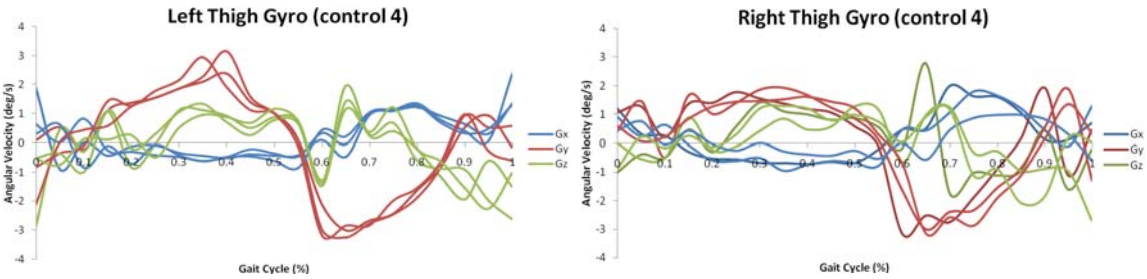
Left Thigh Gyro (control 4)
Angular Velocity (deg/s)
Gait Cycle (%)
Gx
Gy
Gz

Right Thigh Gyro (control 4)
Angular Velocity (deg/s)
Gait Cycle (%)
Gx
Gy
Gz

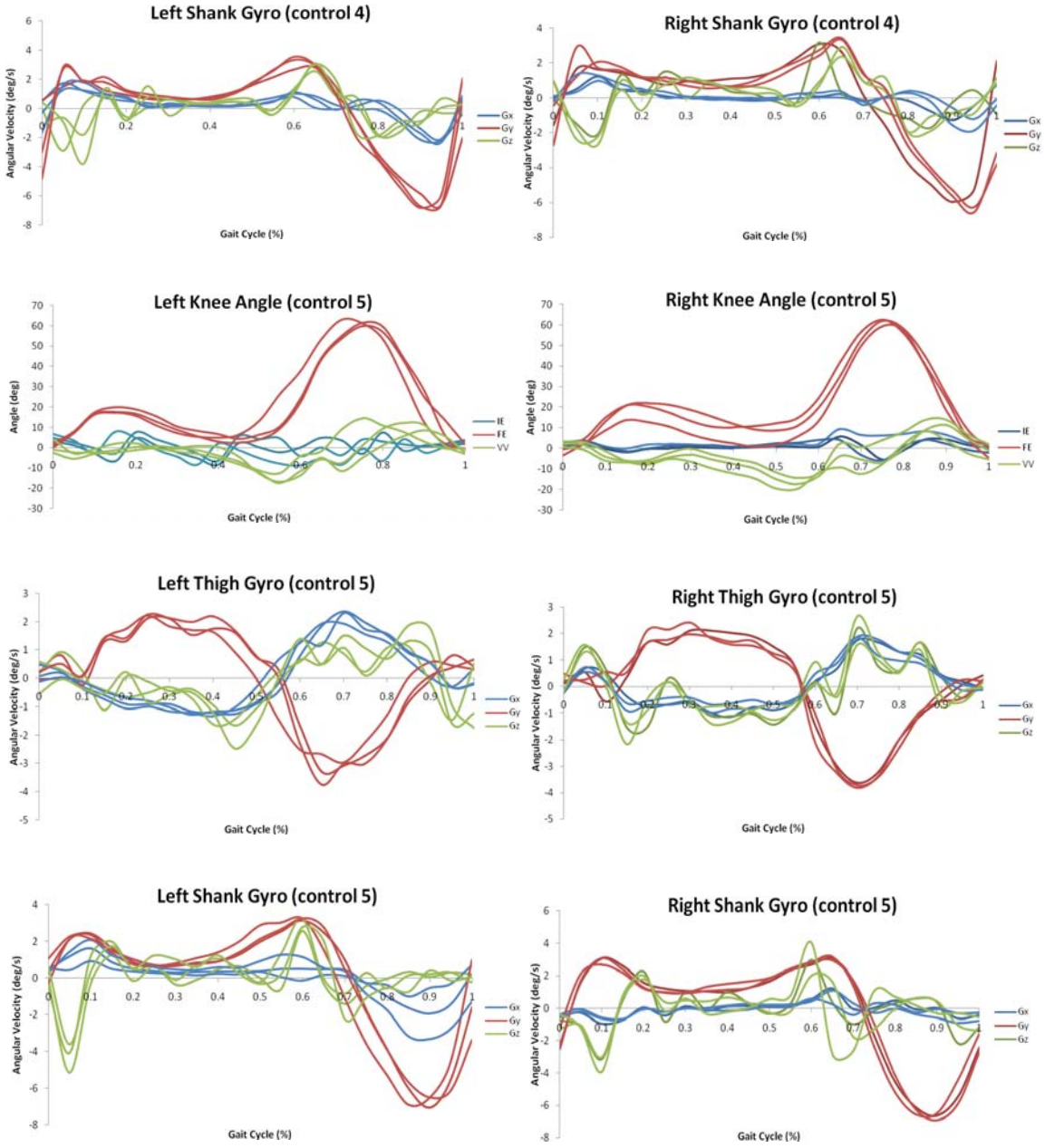

Figures A11-A41: Knee joint angles and thigh/shank angular motions normalized to 100% gait cycle. IE (internal-external rotation), FE (flexion-extension angle), VV (varus-valgus angle), Gx (transverse rotation), Gy (sagittal rotation), Gz (frontal rotation).

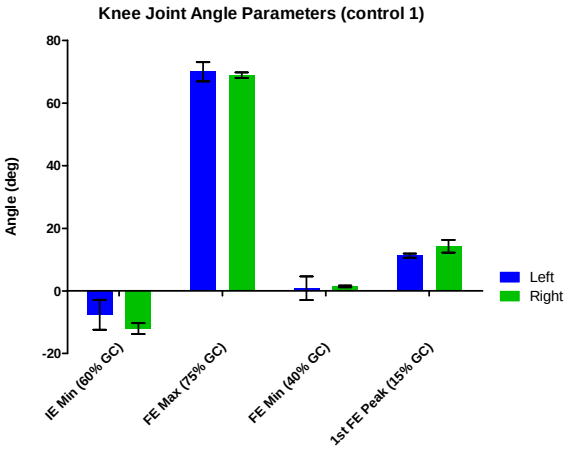
Knee Joint Angle Parameters (control 1)
Angle (deg)
80
60
40
20
0
-20
IE Min (60% GC)
FE Max (75% GC)
FE Min (40% GC)
1st FE Peak (15% GC)
Left
Right

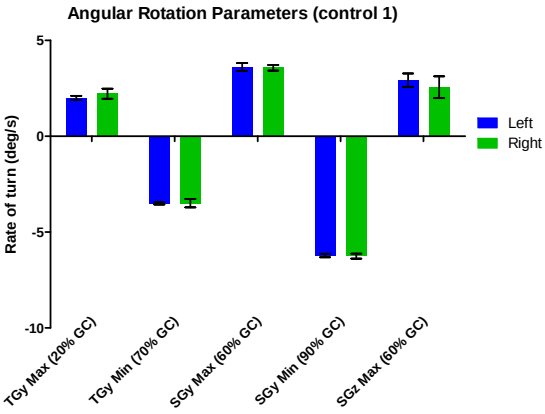
Angular Rotation Parameters (control 1)
Rate of turn (deg/s)
5
0
-5
-10
TGy Max (20% GC)
TGy Min (70% GC)
SGy Max (60% GC)
SGy Min (90% GC)
SGz Max (60% GC)
Left
Right

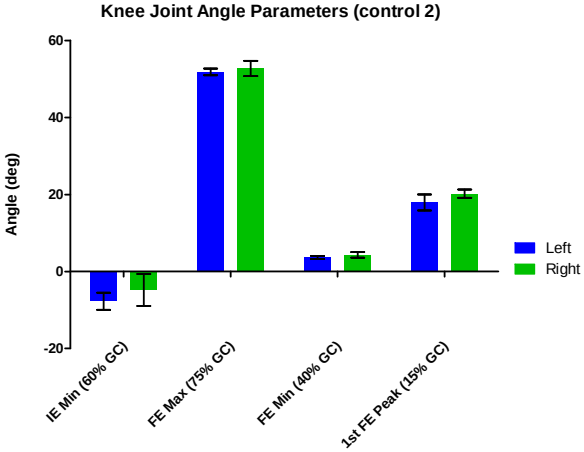
Knee Joint Angle Parameters (control 2)
Angle (deg)
60
40
20
0
-20
IE Min (60% GC)
FE Max (75% GC)
FE Min (40% GC)
1st FE Peak (15% GC)
Left
Right

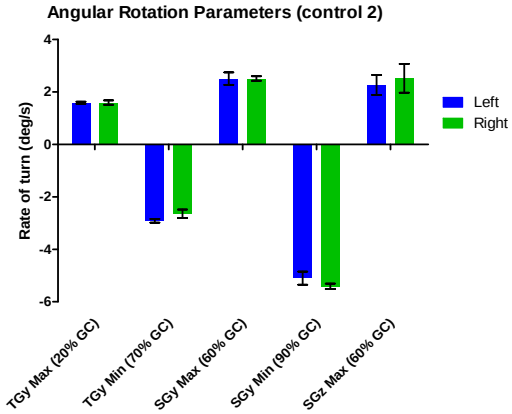
Angular Rotation Parameters (control 2)
Rate of turn (deg/s)
4
2
0
-2
-4
-6
TGy Max (20% GC)
TGy Min (70% GC)
SGy Max (60% GC)
SGy Min (90% GC)
SGz Max (60% GC)
Left
Right

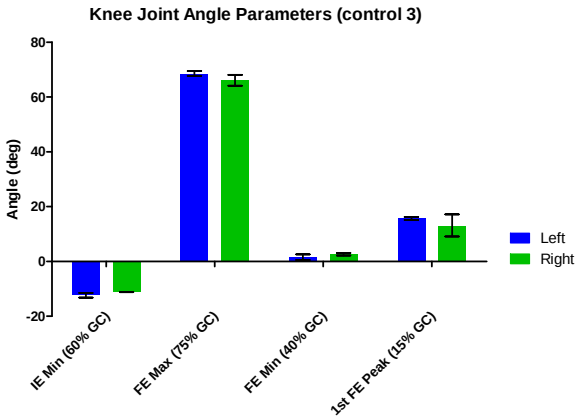
Knee Joint Angle Parameters (control 3)
Angle (deg)
80
60
40
20
0
-20
IE Min (60% GC)
FE Max (75% GC)
FE Min (40% GC)
1st FE Peak (15% GC)
Left
Right

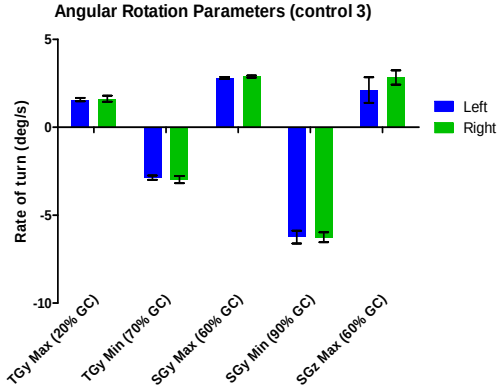
Angular Rotation Parameters (control 3)
Rate of turn (deg/s)
5
0
-5
-10
TGy Max (20% GC)
TGy Min (70% GC)
SGy Max (60% GC)
SGy Min (90% GC)
SGz Max (60% GC)
Left
Right

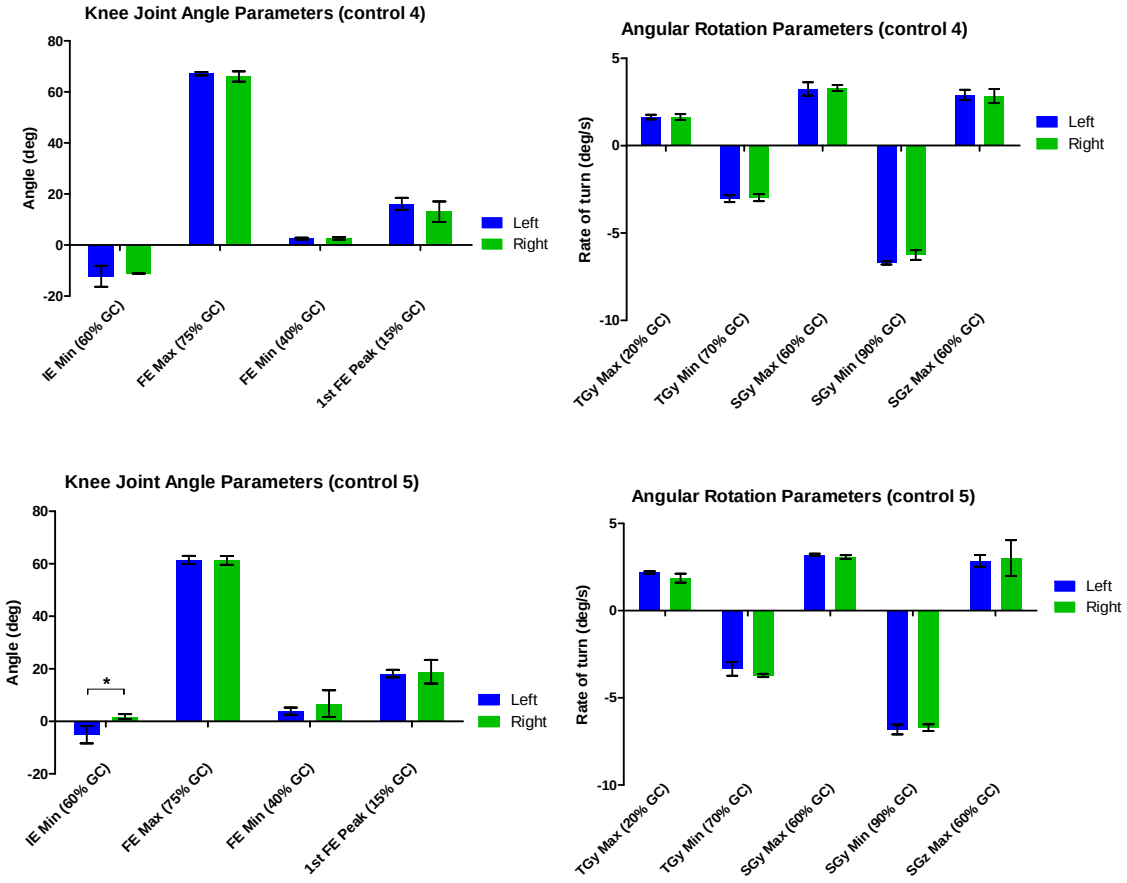

Figures A42-A52: Bar graphs of knee joint angle and angular rotation parameters in a control population. * indicates a significant difference between left and right parameters.

Appendix B

Patient data

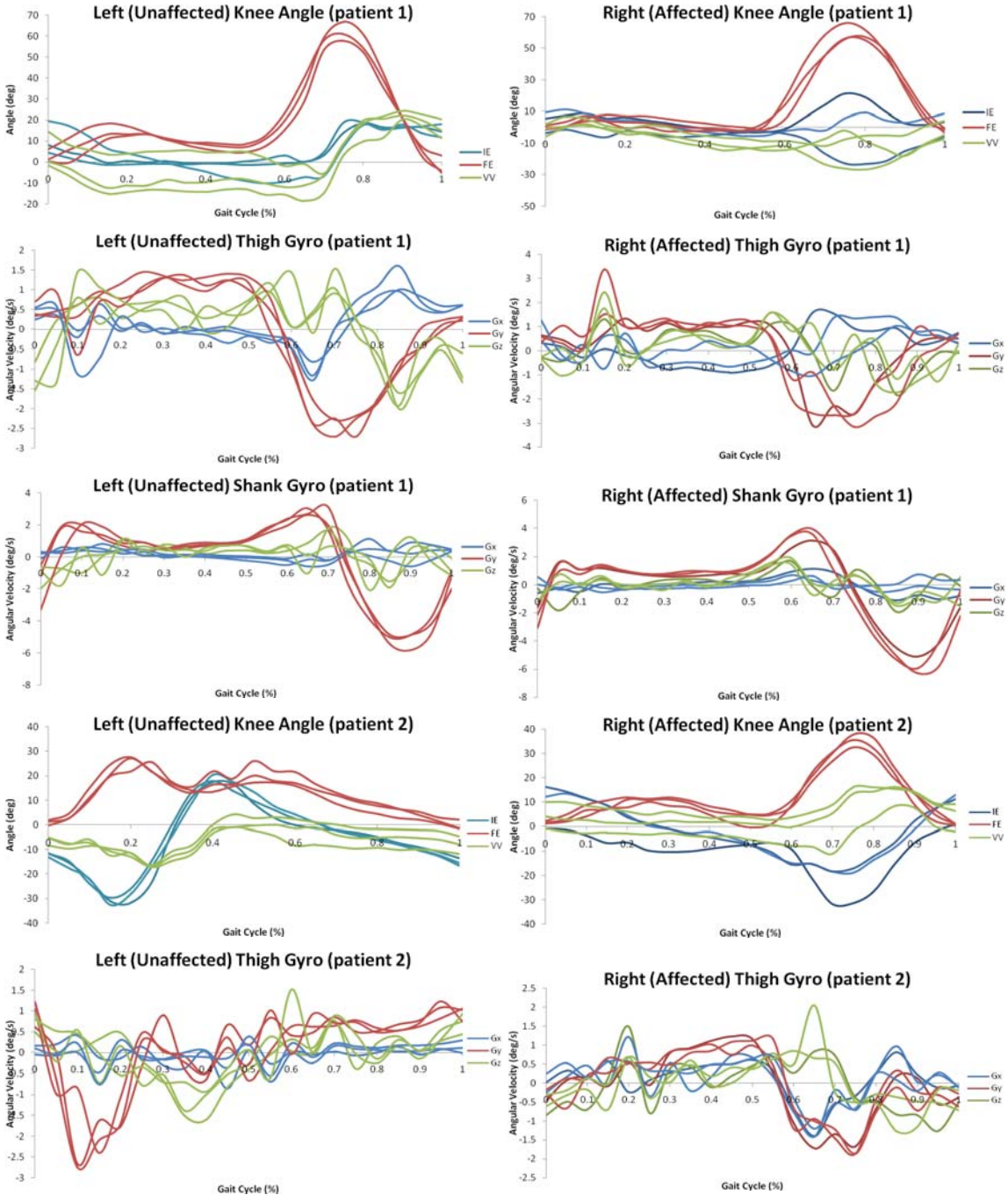

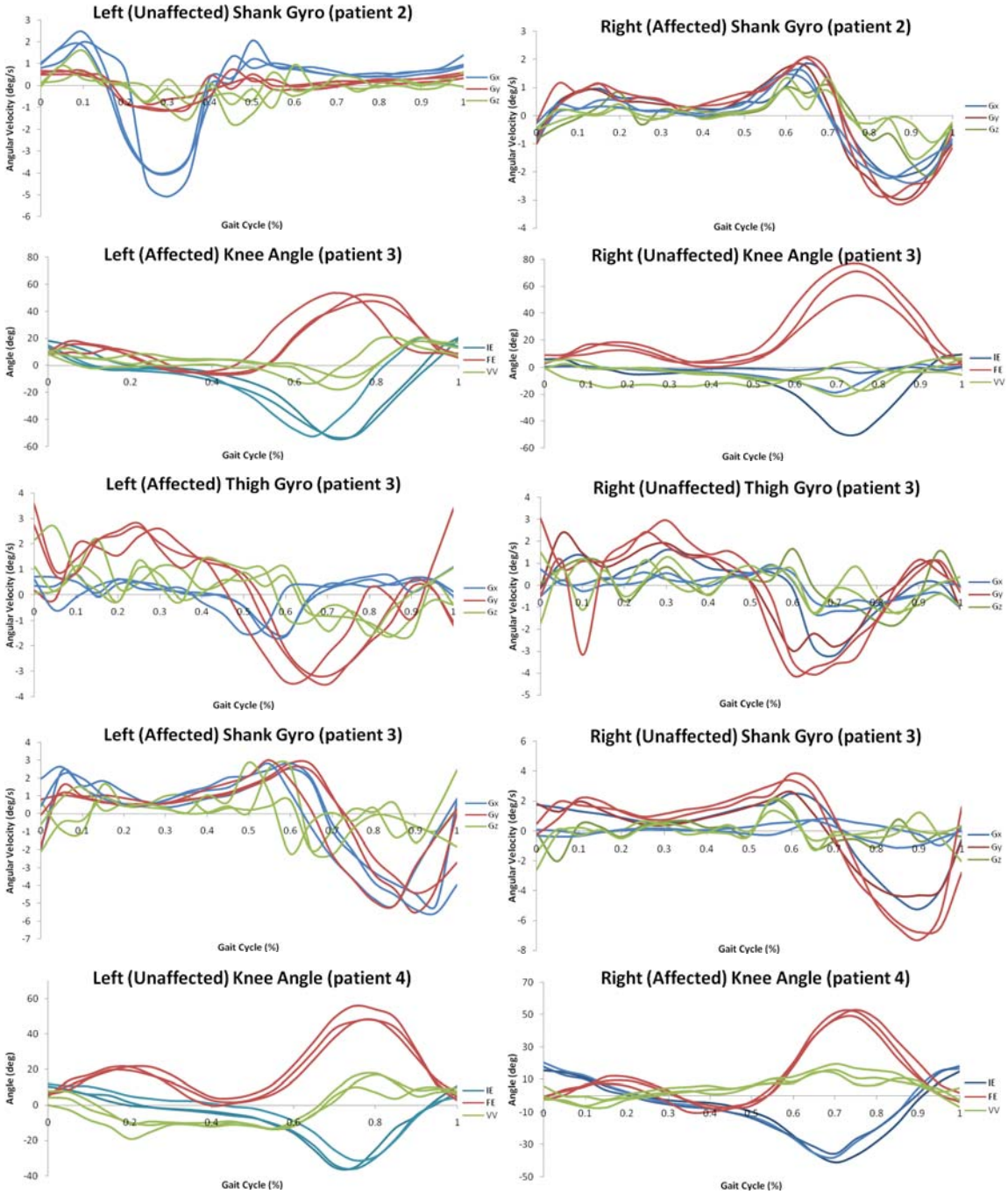
Left (Unaffected) Shank Gyro (patient 2)
Angular Velocity (deg/s)
Gait Cycle (%)
Gx
Gy
Gz
Right (Affected) Shank Gyro (patient 2)
Angular Velocity (deg/s)
Gait Cycle (%)
Gx
Gy
Gz
Left (Affected) Knee Angle (patient 3)
Angle (deg)
Gait Cycle (%)
IE
FE
VV
Right (Unaffected) Knee Angle (patient 3)
Angle (deg)
Gait Cycle (%)
IE
FE
VV
Left (Affected) Thigh Gyro (patient 3)
Angular Velocity (deg/s)
Gait Cycle (%)
Gx
Gy
Gz
Right (Unaffected) Thigh Gyro (patient 3)
Angular Velocity (deg/s)
Gait Cycle (%)
Gx
Gy
Gz
Left (Affected) Shank Gyro (patient 3)
Angular Velocity (deg/s)
Gait Cycle (%)
Gx
Gy
Gz
Right (Unaffected) Shank Gyro (patient 3)
Angular Velocity (deg/s)
Gait Cycle (%)
Gx
Gy
Gz
Left (Unaffected) Knee Angle (patient 4)
Angle (deg)
Gait Cycle (%)
IE
FE
VV
Right (Affected) Knee Angle (patient 4)
Angle (deg)
Gait Cycle (%)
IE
FE
VV

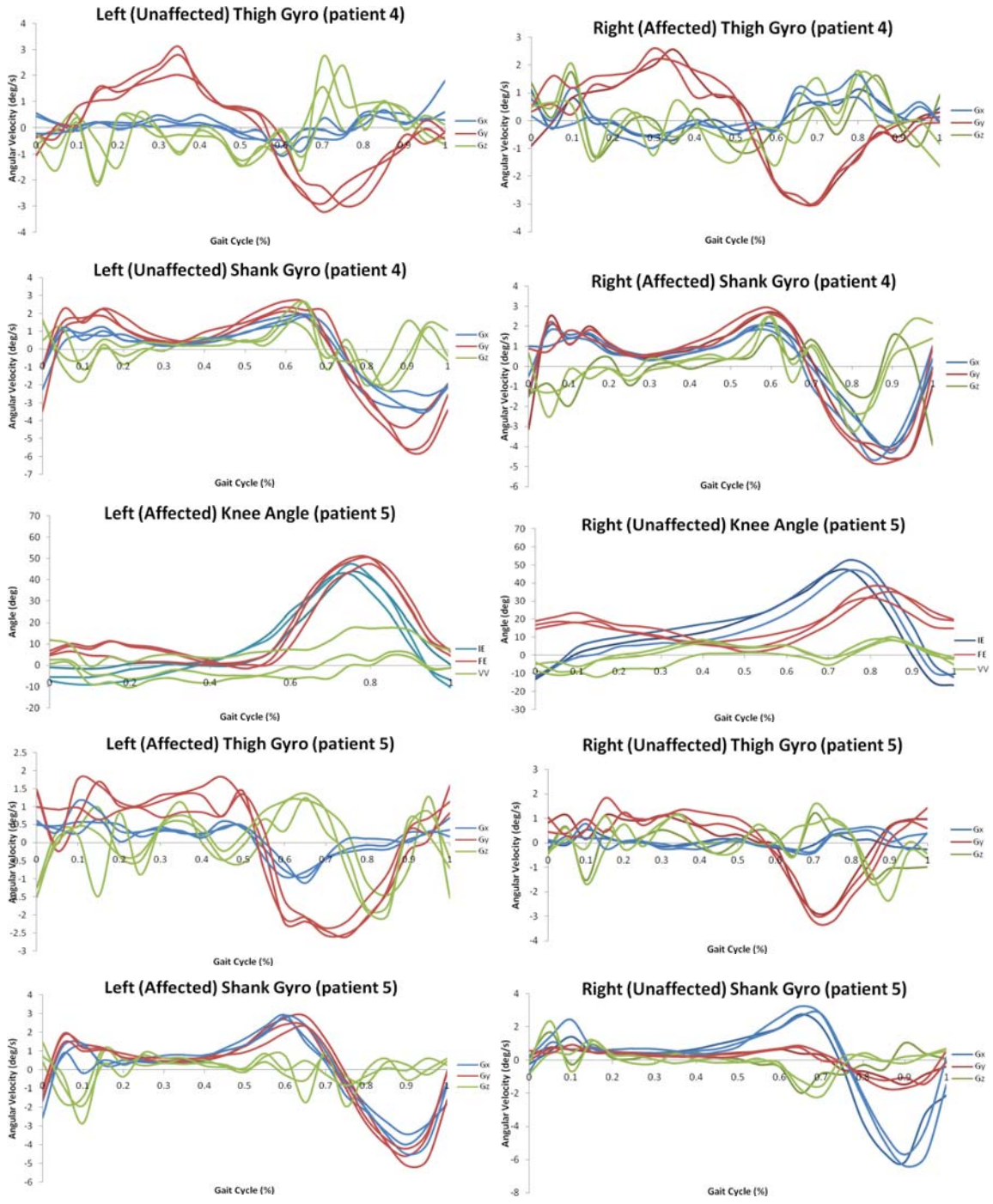

Figures B1-B30: Knee joint angles and thigh/shank angular motions normalized to 100% gait cycle. IE (internal-external rotation), FE (flexion-extension angle), VV (varus-valgus angle), Gx (transverse rotation), Gy (sagittal rotation), Gz (frontal rotation).

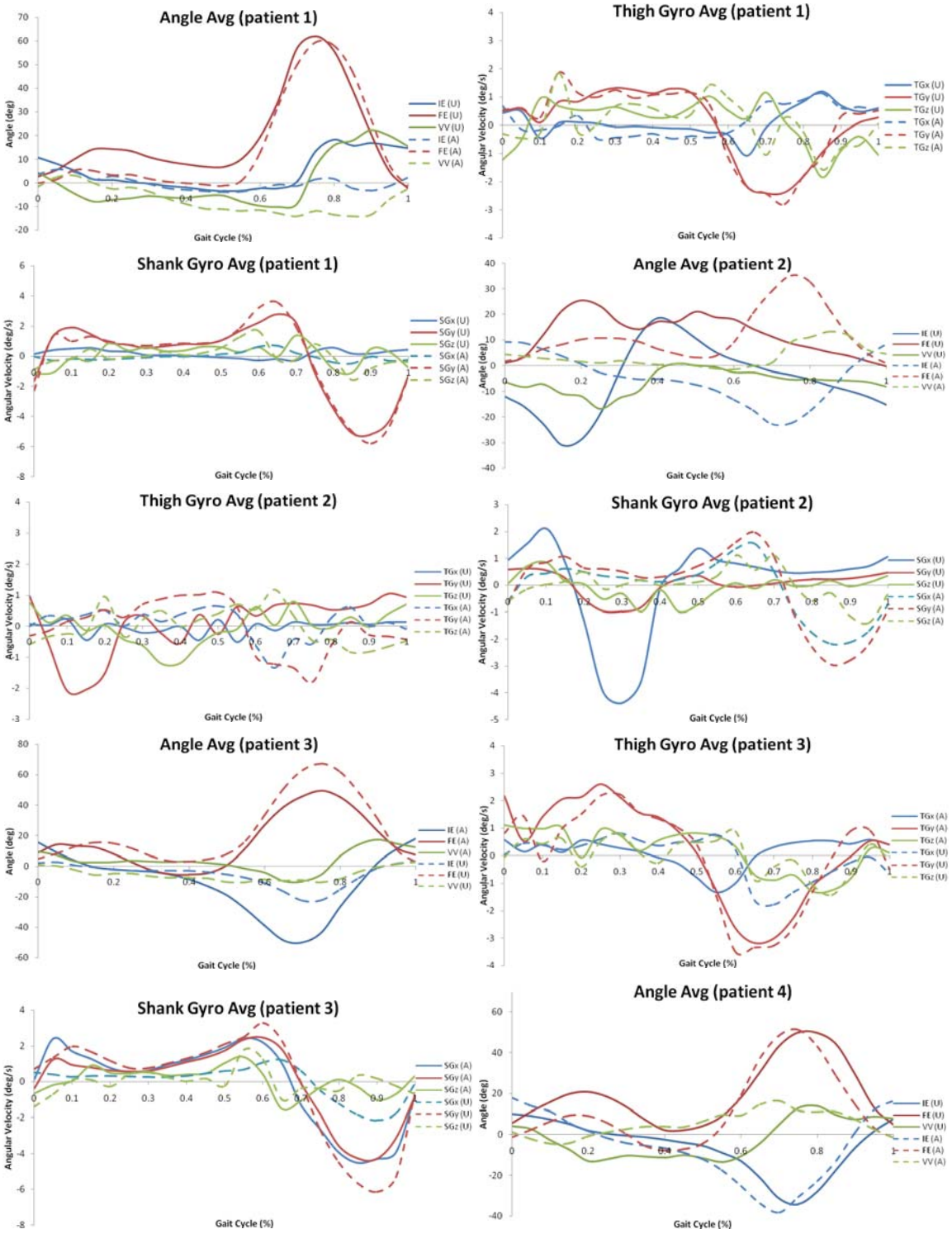
Angle Avg (patient 1)
Angle (deg)
Gait Cycle (%)
IE (U)
FE (U)
VV (U)
IE (A)
FE (A)
VV (A)
Thigh Gyro Avg (patient 1)
Angular Velocity (deg/s)
Gait Cycle (%)
TGx (U)
TGy (U)
TGz (U)
TGx (A)
TGy (A)
TGz (A)
Shank Gyro Avg (patient 1)
Angular Velocity (deg/s)
Gait Cycle (%)
SGx (U)
SGy (U)
SGz (U)
SGx (A)
SGy (A)
SGz (A)
Angle Avg (patient 2)
Angle (deg)
Gait Cycle (%)
IE (U)
FE (U)
VV (U)
IE (A)
FE (A)
VV (A)
Thigh Gyro Avg (patient 2)
Angular Velocity (deg/s)
Gait Cycle (%)
TGx (U)
TGy (U)
TGz (U)
TGx (A)
TGy (A)
TGz (A)
Shank Gyro Avg (patient 2)
Angular Velocity (deg/s)
Gait Cycle (%)
SGx (U)
SGy (U)
SGz (U)
SGx (A)
SGy (A)
SGz (A)
Angle Avg (patient 3)
Angle (deg)
Gait Cycle (%)
IE (A)
FE (A)
VV (A)
IE (U)
FE (U)
VV (U)
Thigh Gyro Avg (patient 3)
Angular Velocity (deg/s)
Gait Cycle (%)
TGx (A)
TGy (A)
TGz (A)
TGx (U)
TGy (U)
TGz (U)
Shank Gyro Avg (patient 3)
Angular Velocity (deg/s)
Gait Cycle (%)
SGx (A)
SGy (A)
SGz (A)
SGx (U)
SGy (U)
SGz (U)
Angle Avg (patient 4)
Angle (deg)
Gait Cycle (%)
IE (U)
FE (U)
VV (U)
IE (A)
FE (A)
VV (A)

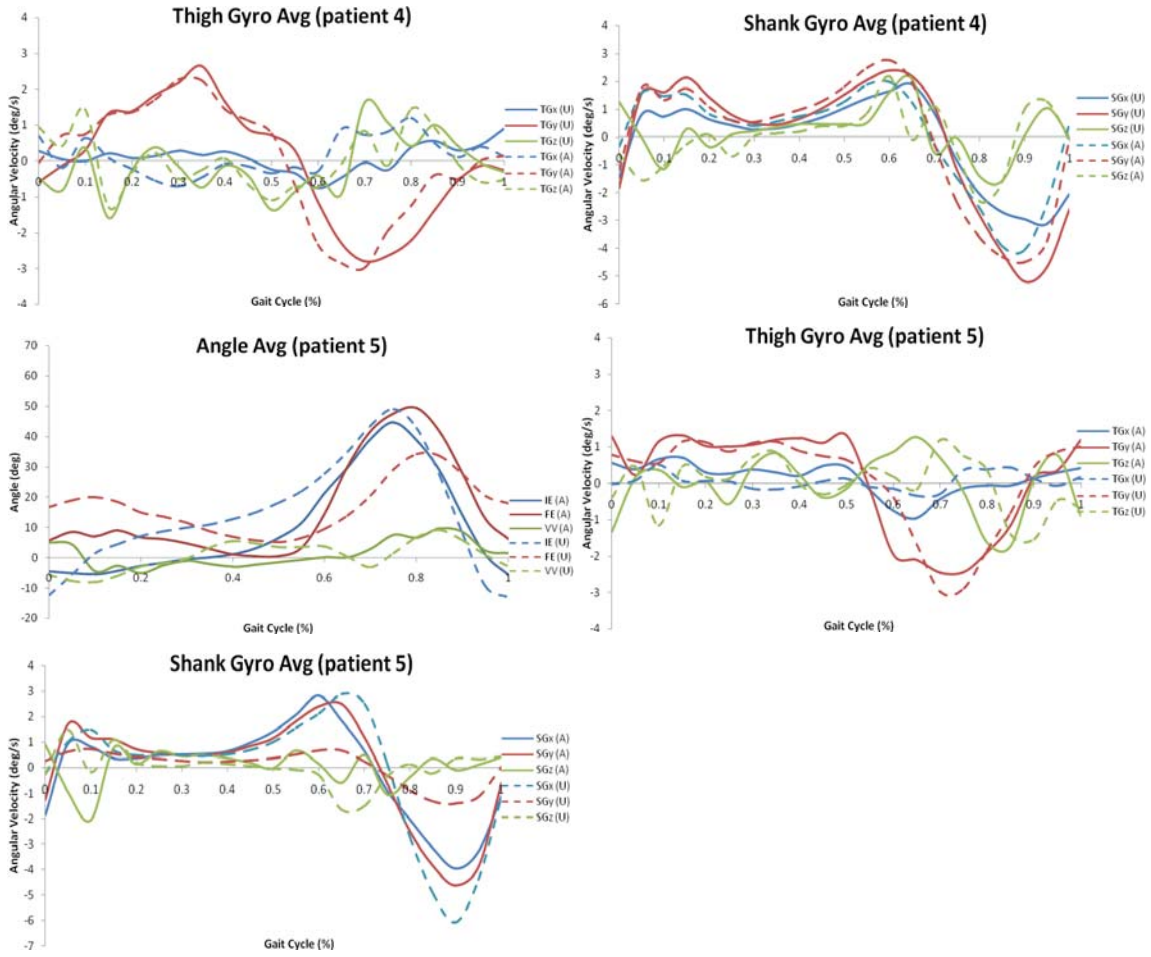

Figures B31-B45: Superimposed unaffected and affected limb kinematic averages. Solid lines represent unaffected limb data and dashed lines represent affected limb data.

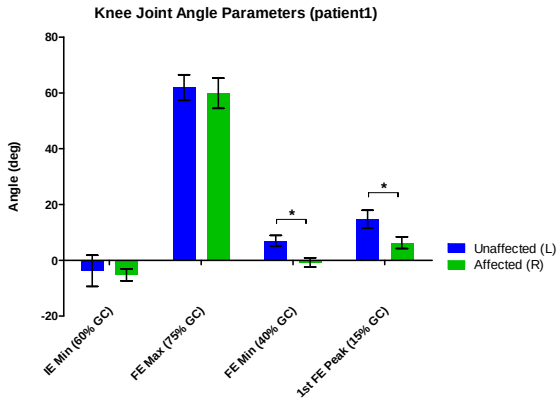
Knee Joint Angle Parameters (patient1)
Angle (deg)
80
60
40
20
0
-20
*
*
*
IE Min (60% GC)
FE Max (75% GC)
FE Min (40% GC)
1st FE Peak (15% GC)
Unaffected (L)
Affected (R)

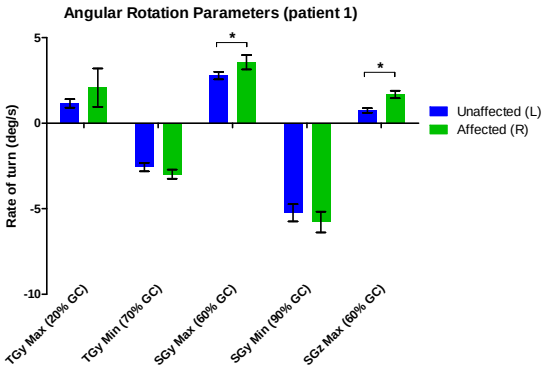
Angular Rotation Parameters (patient 1)
Rate of turn (deg/s)
5
0
-5
-10
*
*
*
TGy Max (20% GC)
TGy Min (70% GC)
SGy Max (60% GC)
SGy Min (90% GC)
SGz Max (60% GC)
Unaffected (L)
Affected (R)

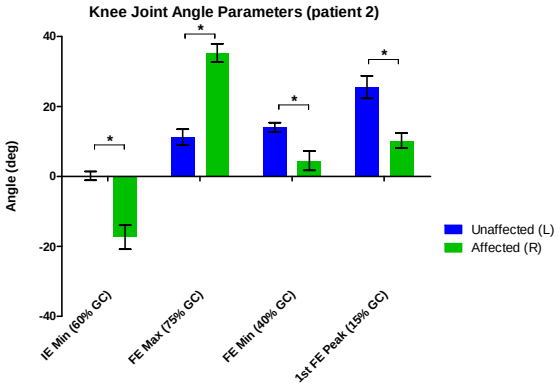
Knee Joint Angle Parameters (patient 2)
Angle (deg)
40
20
0
-20
-40
*
*
*
*
IE Min (60% GC)
FE Max (75% GC)
FE Min (40% GC)
1st FE Peak (15% GC)
Unaffected (L)
Affected (R)

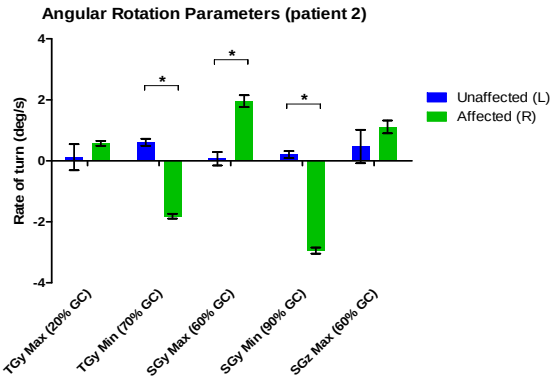
Angular Rotation Parameters (patient 2)
Rate of turn (deg/s)
4
2
0
-2
-4
*
*
*
TGy Max (20% GC)
TGy Min (70% GC)
SGy Max (60% GC)
SGy Min (90% GC)
SGz Max (60% GC)
Unaffected (L)
Affected (R)

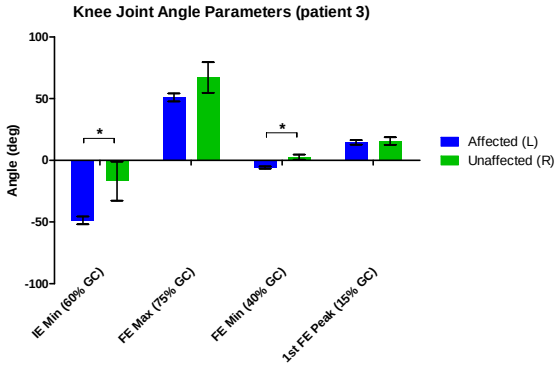
Knee Joint Angle Parameters (patient 3)
Angle (deg)
100
50
0
-50
-100
*
*
IE Min (60% GC)
FE Max (75% GC)
FE Min (40% GC)
1st FE Peak (15% GC)
Affected (L)
Unaffected (R)

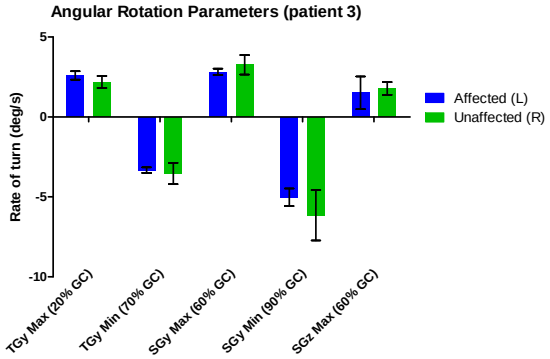
Angular Rotation Parameters (patient 3)
Rate of turn (deg/s)
5
0
-5
-10
TGy Max (20% GC)
TGy Min (70% GC)
SGy Max (60% GC)
SGy Min (90% GC)
SGz Max (60% GC)
Affected (L)
Unaffected (R)

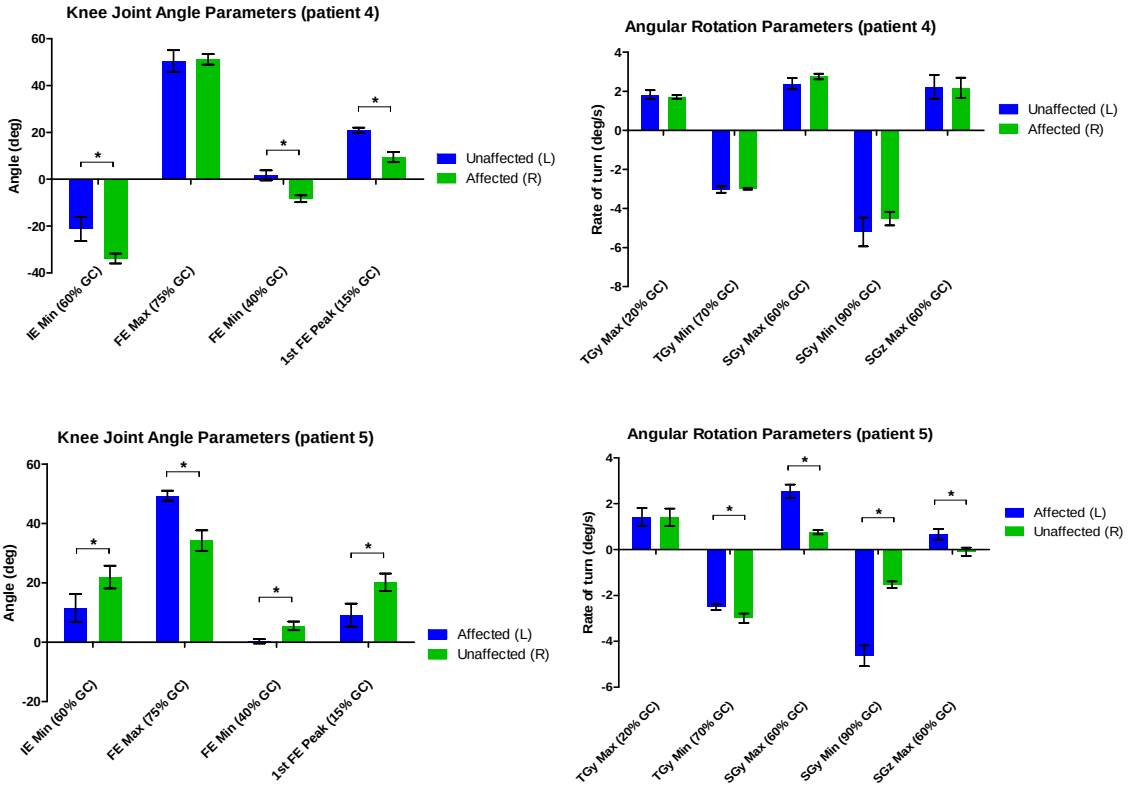

Figures B46-B56: Bar graphs of knee joint angle and angular rotation parameters in an acute antalgic gait population. * indicates a significant difference between affected and unaffected limb parameters.

Tables B1-B5: Functionality ratio score card for all patients. Red shading indicates parameters previously calculated as significantly different between limbs.

Patient 1		*Unaffected Limb (L)*	*Affected Limb (R)*	*Normal functional range*
TGy Max (20±5% GC)	Mean	1.163	2.081	
	Ratio	1.790		(0.899 – 1.177)
TGy Min (70±5% GC)	Mean	-2.565	-2.980	
	Ratio	1.162		(0.897 – 1.102)
SGy Max (60±5% GC)	Mean	2.791	3.565	
	Ratio	1.277		(0.970 – 1.048)
SGy Min (90±5% GC)	Mean	-5.236	-5.777	
	Ratio	1.103		(0.942 – 1.072)
FE Max (75±5% GC)	Mean	61.919	59.866	
	Ratio	0.967		(0.983 – 1.037)
FE Min (40±5% GC)	Mean	7.000	-0.743	
	Ratio	-0.106		(0.570 – 0.982)
FE Peak (15±5% GC)	Mean	14.706	6.337	
	Ratio	0.431		(0.790 – 1.238)

Patient 2		*Unaffected Limb (L)*	*Affected Limb (R)*	*Normal functional range*
TGy Max (20±5% GC)	Mean	0.122	0.575	
	Ratio	4.723		(0.899 – 1.177)
TGy Min (70±5% GC)	Mean	0.607	-1.814	
	Ratio	-2.986		(0.897 – 1.102)
SGy Max (60±5% GC)	Mean	0.069	1.960	
	Ratio	28.411		(0.970 – 1.048)
SGy Min (90±5% GC)	Mean	0.205	-2.945	
	Ratio	-14.343		(0.942 – 1.072)
FE Max (75±5% GC)	Mean	11.215	35.262	
	Ratio	3.144		(0.983 – 1.037)
FE Min (40±5% GC)	Mean	14.043	4.466	
	Ratio	0.318		(0.570 – 0.982)
FE Peak (15±5% GC)	Mean	25.528	10.285	
	Ratio	0.403		(0.790 – 1.238)

Patient 3		*Affected Limb (L)*	*Unaffected Limb (R)*	*Normal functional range*
TGy Max (20±5% GC)	Mean	2.600	2.188	
	Ratio	1.188		(0.899 – 1.177)
TGy Min (70±5% GC)	Mean	-3.327	-3.540	
	Ratio	0.940		(0.897 – 1.102)
SGy Max (60±5% GC)	Mean	2.824	3.267	
	Ratio	0.864		(0.970 – 1.048)
SGy Min (90±5% GC)	Mean	-5.024	-6.153	
	Ratio	0.996		(0.942 – 1.072)
FE Max (75±5% GC)	Mean	50.909	67.105	
	Ratio	0.759		(0.983 – 1.037)
FE Min (40±5% GC)	Mean	-5.824	2.504	
	Ratio	-2.326		(0.570 – 0.982)
FE Peak (15±5% GC)	Mean	14.526	15.635	
	Ratio	0.929		(0.790 – 1.238)

Patient 4		*Unaffected Limb (L)*	*Affected Limb (R)*	*Normal functional range*
TGy Max (20±5% GC)	Mean	1.831	1.714	
	Ratio	0.936		(0.899 – 1.177)
TGy Min (70±5% GC)	Mean	-3.030	-2.987	
	Ratio	0.986		(0.897 – 1.102)
SGy Max (60±5% GC)	Mean	2.393	2.759	
	Ratio	1.153		(0.970 – 1.048)
SGy Min (90±5% GC)	Mean	-5.201	-4.520	
	Ratio	0.869		(0.942 – 1.072)
FE Max (75±5% GC)	Mean	50.452	51.219	
	Ratio	1.015		(0.983 – 1.037)
FE Min (40±5% GC)	Mean	1.698	-8.277	
	Ratio	-4.875		(0.570 – 0.982)
FE Peak (15±5% GC)	Mean	20.940	9.453	
	Ratio	0.451		(0.790 – 1.238)

Patient 5		*Affected Limb (L)*	*Unaffected Limb (R)*	*Normal functional range*
TGy Max (20±5% GC)	Mean	1.422	1.404	
	Ratio	1.013		(0.899 – 1.177)
TGy Min (70±5% GC)	Mean	-2.515	-2.986	
	Ratio	0.842		(0.897 – 1.102)
SGy Max (60±5% GC)	Mean	2.540	0.758	
	Ratio	3.350		(0.970 – 1.048)
SGy Min (90±5% GC)	Mean	-4.627	-1.529	
	Ratio	3.026		(0.942 – 1.072)
FE Max (75±5% GC)	Mean	49.356	34.230	
	Ratio	1.442		(0.983 – 1.037)
FE Min (40±5% GC)	Mean	0.342	5.517	
	Ratio	0.062		(0.570 – 0.982)
FE Peak (15±5% GC)	Mean	9.118	20.168	
	Ratio	0.452		(0.790 – 1.238)

REFERENCES

[1] Andriacchi, T.P., et al., Patellofemoral design influences function following total knee arthroplasty. *J Arthroplasty*, 1997. **12**: p. 243-9.

[2] Catani, F., et al., Mobile and fixed bearing total knee prosthesis functional comparison during stair climbing. *Clin Biomech*, 2003. **18**: p. 410-8.

[3] Kaufman, K.R., et al., Gait characteristics of patients with knee osteoarthritis. *J Biomech*, 2001. **34**: p. 907-15.

[4] Minns, R.J., The role of gait analysis in the management of the knee. *Knee*, 2005. **12**: p. 157-62.

[5] Smith, A.J., et al., A kinematic and kinetic analysis of walking after total knee arthroplasty with and without patellar resurfacing. *Clin Biomech*, 2006. **21**: p. 379-86.

[6] Solak, S.A., et al., Does bilateral total knee arthroplasty affect gait in women? *J Arthroplasty*, 2005. **20**: p. 745-50.

[7] Webster, K.E., et al., Quantitative gait analysis after medial unicompartmental knee arthroplasty for osteoarthritis. *J Arthroplasty*, 2003. **18**: p. 751-9.

[8] Rubino, F.A., Gait disorders. *Neurologist*, 2002. **8**: p. 254-62.

[9] Gage, J.R., An overview of normal walking. *Instr Course Lect*, 1990. **39**: p. 291-303.

[10] Lim, M.R., et al., Evaluation of the elderly patient with an abnormal gait. *J Am Acad Orthop Surg*, 2007. **15**: p. 107-17.

[11] Herr, H., and Wilkenfeld, A., User-adaptive control of a magnetorheological prosthetic knee. *Ind Robot*, 2003. **3**: p. 42-55.

[12] Perry, J., Gait analysis: normal and pathological function. Thorofare, NJ: Slack Inc., 1992.

[13] Insall, J.N., et al., A comparison of four models of total knee-replacement prosthesis. *J Bone Joint Surg*, 1976. **58**: p. 754-65.

[14] Insall, J.N., et al., Rationale of the Knee Society clinical rating system. *Clin Orthop Relat Res*, 1989. **Nov**: p. 13-4.

[15] Bach, C.M., et al., Scoring systems in total knee arthroplasty. *Clin Orthop Relat Res*, 2002. **Jun**: p. 184-96.

[16] Konig, A., et al., The need for a dual rating system in total knee arthroplasty. *Clin Orthop Relat Res*, 1997. **Dec**: p. 161-7.

[17] Lieberman, J.R., et al., Outcome after total hip arthroplasty: comparison of a traditional disease-specific and a quality-of-life measurement of outcome. *J Arthroplasty*, 1997. **12**: p. 639-45.

[18] Lindemann, U., et al., Gait analysis and WOMAC are complementary in assessing functional outcome in total hip replacement. *Clin Rehabil*, 2006. **20**: p. 413-20.

[19] Kramers-de Quervain, I.A., et al., Quantitative gait analysis after bilateral total knee arthroplasty with two different systems within each subject. *J Arthroplasty*, 1997. **12**: p. 168-79.

[20] Molet, T., et al., Human motion capture driven by orientation measurements. *Presence-Teleop Virt*, 1999. **8**: p. 187-203.

[21] Richards, J.G., The measurement of human motion: a comparison of commercially available systems. *Hum Movement Sci*, 1999. **18**: p. 589-602.

[22] Sutherland, D.H., The evolution of clinical gait analysis: part II kinematics. *Gait Posture*, 2002. **16**: p. 159-79.

[23] Cappozzo, A., et al., Surface-marker cluster design criteria for 3-D bone movement reconstruction. *IEEE Trans Biomed Eng*, 1997. **44**: p. 1165-74.

[24] Cappozzo, A., et al., Position and orientation in space of bones during movement: anatomical frame definition and determination. *Clin Biomech*, 1995. **10**: p. 171-8.

[25] Cappozzo, A., et al., Position and orientation in space of bones during movement: experimental artefacts. *Clin Biomech*, 1996. **11**: p. 90-100.

[26] Ramsey, D.K. and P.F. Wretenberg, Biomechanics of the knee: methodological considerations in the in vivo kinematic analysis of the tibiofemoral and patellofemoral joint. *Clin Biomech*, 1999. **14**: p. 595-611.

[27] Dejnabadi, H., et al., A new approach to accurate measurement of uniaxial joint angles based on a combination of accelerometers and gyroscopes. *IEEE Trans Biomed Eng*, 2005. **52**: p. 1478-84.

[28] Aminian, K., et al., Spatio-temporal parameters of gait measured by an ambulatory system using miniature gyroscopes. *J Biomech*, 2002. **35**: p. 689-99.

[29] Najafi, B., et al., Ambulatory system for human motion analysis using a kinematic sensor: monitoring of daily physical activity in the elderly. *IEEE Trans Biomed Eng*, 2003. **50**: p. 711-23.

[30] Aminian, K., et al., Physical activity monitoring based on accelerometry: validation and comparison with video observation. *Med Biol Eng Comput*, 1999. **37**: p. 304-8.

[31] Roetenberg, D., et al., Ambulatory position and orientation tracking fusing magnetic and inertial sensing. *IEEE Trans Biomed Eng*, 2007. **54**: p. 883-90.

[32] Luinge, H.J. and P.H. Veltink, Inclination measurement of human movement using a 3-D accelerometer with autocalibration. *IEEE Trans Neural Syst Rehabil Eng*, 2004. **12**: p. 112-21.

[33] Luinge, H.J. and P.H. Veltink, Measuring orientation of human body segments using miniature gyroscopes and accelerometers. *Med Biol Eng Comput*, 2005. **43**: p. 273-82.

[34] Mayagoitia, R.E., et al., Accelerometer and rate gyroscope measurement of kinematics: and inexpensive alternative to optical motion analysis systems. *J Biomech*, 2002. **35**: p. 537-42.

[35] Aminian, K. and B. Najafi, Capturing human motion using body-fixed sensors: outdoor measurement and clinical applications. *Comput Animat Virt W*, 2004. **15**: p. 79-94.

[36] Tong, K. and N.H. Granat, A practical gait analysis system using gyroscopes. *Med Eng Phys*, 1999. **21**: p. 87-94.

[37] Mayagoitia, R.E., et al., Standing balance evaluation using a triaxial accelerometer. *Gait Posture*, 2002. **16**: p. 55-9.

[38] Morris, J.R., Accelerometery: a technique for the measurement of human body movements. *J Biomech*, 1973. **6**: p. 729-36.

[39] Heyn, A., et al., The kinematics of the swing phase obtained from accelerometer and gyroscope measurements. *Engineering in Medicine and Biology Society*, 1996. **462**: p. 463-4.

[40] Xsens Motion Technologies: www.xsens.com.

[41] Koslin, A.J., Validation of an inertial sensor system for quantifying knee function. Master's thesis, Dept. of Bioengineering, 2006. Clemson University, Clemson, SC, United States.

[42] Ostchega, Y., et al., The prevalence of functional limitations and disability in older persons in the US: data from the National Health and Nutrition Examination Survey III. *J Am Geriatr Soc*, 2000. **48**: p. 1132-5.

[43] Hough, J.C., et al., Gait disorders in the elderly. *Am Fam Pract*, 1987. **30**: p. 191-6.

[44] Kawano, K., et al., Analyzing 3D Knee Kinematics Using Accelerometers, Gyroscopes and Magnetometers. *System of Systems Engineering*, 2007. *SoSE '07, IEEE International Conference*. p. 1-6.

[45] Goodvin, C.I., Development of a real-time spinal motion inertial measurement system for vestibular disorder application. Master's thesis, Dept. of Mechanical Engineering, 2003. University of Victoria, Victoria, BC, Canada.

[46] Winter, D.A., Human balance and posture control during standing and walking. *Gait Posture*, 1995. **3**: p. 193-214.

[47] Duhamel, A., et al., Statistical tools for clinical gait analysis. *Gait Posture*, 2004. **20**: p. 204-12.